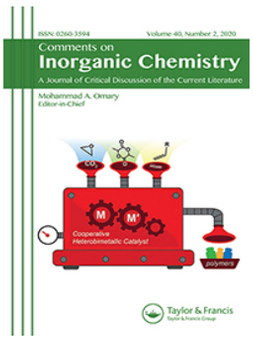

Comments on Inorganic Chemistry

A Journal of Critical Discussion of the Current Literature

ISSN: 0260-3594 (Print) 1548-9574 (Online) Journal homepage: https://www.tandfonline.com/loi/gcic20

Photocatalysis with Transition Metal Based Photosensitizers

Jong-Hwa Shon & Thomas S. Teets

To cite this article: Jong-Hwa Shon & Thomas S. Teets (2020) Photocatalysis with Transition Metal Based Photosensitizers, Comments on Inorganic Chemistry, 40:2, 53-85, DOI: 10.1080/02603594.2019.1694517

To link to this article: https://doi.org/10.1080/02603594.2019.1694517

Published online: 18 Dec 2019.

COMMENTS ON INORGANIC CHEMISTRY
2020, VOL. 40, NO. 2, 53–85
https://doi.org/10.1080/02603594.2019.1694517

Taylor & Francis
Taylor & Francis Group

Photocatalysis with Transition Metal Based Photosensitizers

Jong-Hwa Shon and Thomas S. Teets

Department of Chemistry, University of Houston, Houston, TX, USA

ABSTRACT

Photocatalysis under visible-light irradiation has many applications in organic synthesis and solar fuels. Out of the many photosensitizers that have been used in photocatalysis applications, metal-based photosensitizers are most prominent, given their excellent tunability and performance. In this review, different categories of metal-based photosensitizers are summarized and their function in photocatalytic reactions is described. There are also examples of recently developed photocatalytic applications using these photosensitizers.

KEYWORDS

Photocatalysis; photoredox catalysis; photosensitizer; photoinduced electron transfer

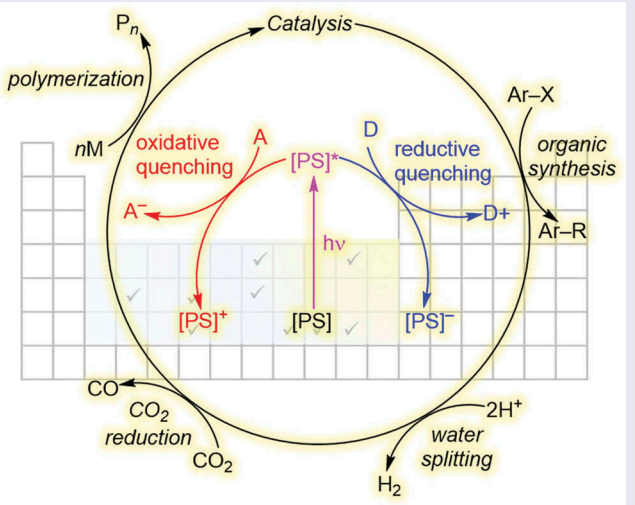

1. Introduction

A photosensitizer (PS) is a compound, which absorbs photon energy, usually from the UVA to visible light region, and after excitation either participates in energy or electron transfer. Taking advantage of these properties, there is intensive research in displays[1,2], sensing[3,4], energy harvesting[5–10], and

CONTACT Thomas S. Teets tteets@uh.edu Department of Chemistry, University of Houston, 3585 Cullen Blvd. Room 112, Houston, TX 77204-5003

Color versions of one or more of the figures in the article can be found online at www.tandfonline.com/gcic.

photo-initiated chemical reactions.[11–15] Photoredox catalysis or photocatalysis is one capacity of photosensitizers which uses the photon energy as an additional driving force for a chemical reaction, such as activation of a redox-active organic molecule for organic synthesis, activation of a water molecule for hydrogen gas generation, or reduction of a carbon dioxide molecule. Such catalytic applications are one of the primary applications of molecular photosensitizers. The major advantage of using a photosensitizer as a catalyst is that the thermodynamic and kinetic driving force of the reaction is gained from external light energy as opposed to thermal energy. Thus, ideal photocatalysis can be controlled in an ON-OFF fashion and is particularly beneficial for transformations that are thermodynamically unfavorable or kinetically sluggish in the dark.

There are several types of photosensitizers for photocatalysis, including organic dyes and semiconducting materials, but photosensitizers based on coordination compounds are especially prominent for photocatalysis. Metal-based coordination complexes with conjugated ligands typically are strong visible-light absorbers, which has spurred their development in photoredox applications. Ruthenium-based coordination complexes are historically the most intensely researched class of molecular photosensitizers. Some of the earliest research in photoinduced electron-transfer or photocatalysis used the complex $[Ru(bpy)_3]^{2+}$ (bpy = 2,2′-bipyridine)[16,17], which remains prominent in recent organic synthesis applications. Since the early work with $[Ru(bpy)_3]^{2+}$ there has been a considerable effort in the development of new photosensitizers, both for fundamental studies of excited-state energy and charge transfer and for photocatalysis. Even though there is a wide variety of candidate photosensitizers for photocatalysis, the reaction is limited by the redox properties of the photosensitizer, which means the substrates or cocatalysts that can be activated are dictated by the photosensitizer's redox potentials. Thus, much current research in photosensitizer design focuses on controlling the ground- and excited-state redox properties of photosensitizers by changing the metal and/or the ligand design. Such structure–property relationships are crucial for designing improved photosensitizers and for selecting the correct photosensitizer for a particular application. The redox properties of the photosensitizer dictate not only the thermodynamic aspects of photocatalytic reactions but are also key components in determining reaction kinetics. According to the Marcus electron-transfer theory,[18,19] stronger reducing or oxidizing ability leads to faster rates of electron transfer in the Marcus normal region, and *vice versa* in the Marcus inverted region. Thus, there is no standard photosensitizer for all photocatalytic reactions, and the preparation of photocatalyst libraries with a large window of redox potentials and excited-state properties will be critical for continued advances in photocatalysis research.

This review describes some of the most important classes of molecular metal-containing photosensitizers. Specifically, we focus on compounds that

undergo *outer-sphere* electron-transfer reactions following visible-light excitation; we do not attempt in this review to summarize the many examples of *inner-sphere* photochemistry that have been developed in coordination compounds. In the first part of the review, some of the principles of photoinduced redox processes are outlined, with the majority of the review cataloging different categories of photosensitizers that have been developed. This survey of photosensitizer structure types is not designed to be comprehensive, but rather is intended to provide a concise summary of some of the major categories of metal-based photosensitizers, focusing on recent developments but providing historical context where needed. Our own group's research involves the design of cyclometalated iridium photoreductants,[20,21] one of the most prominent classes of photosensitizers in the synthetic chemistry literature, so we do place a larger emphasis on these compounds but also include photosensitizers of several other transition metals to give a sense of the breadth of this field. Furthermore, we place most of the attention on molecules that have been used as *photoreductants*, although the redox potentials associated with photooxidiation are also provided where available. In the final part of the article, we summarize a few select photocatalytic transformations where some of the aforementioned photosensitizers have found utility, giving a small sampling of the diverse range of transformations these photosensitizers can promote. Since the major focus of this review is photoreductants, the catalytic transformations we describe are all either net reductive transformations or are initiated by electron transfer from the photosensitizer. We include examples from solar fuels, organic synthesis, and polymer chemistry to highlight the wide range of applications of photoinduced electron transfer. In addition, in all of the chosen examples, the role of the photosensitizer is clearly identified, and with these few case studies, the reader will appreciate the diverse ways in which photoinduced redox chemistry can be used to promote chemical transformations of interest.

2. Mechanism of photocatalysis

2.1. *Photocatalysis via photoinduced-electron transfer (PET)*

Mechanisms of photocatalysis are classified by the role of the photosensitizer in the reaction, primarily as an electron donor or acceptor via outer-sphere electron transfer, or via an energy-transfer pathway. Electron transfer (ET) mechanisms in the ground state are well defined by the Marcus ET theory. The kinetics of electron transfer in the excited-state, also known as photoinduced electron-transfer (PET), is also governed by the same Marcus relationship with the addition of a term for the photosensitizer's excited-state energy, typically the triplet excited-state energy for metal-based photosensitizers.[22] In the Marcus electron-transfer theory, the rate of adiabatic outer-sphere ET is described by Equation (1).

$$k_{ET} = \left(\frac{k_B T}{h}\right) \exp\left[\frac{-(\lambda + \Delta G_0)^2}{4\lambda k_B T}\right] \quad (1)$$

where h is Planck's constant, k_B is the Boltzmann constant, T is temperature (K), λ is the reorganization energy, and ΔG_0 is the driving force of the electron-transfer reaction.

The driving force of the ET reaction (ΔG_0) depends on the difference between standard redox potentials of the electron donor (D) and the acceptor (A). Similarly, in PET, the kinetics also follows Equation (1) except the driving force is given by Equation (2), which includes the excited-state energy E(PS*) of the photosensitizer in addition to the redox potentials of the donor and acceptor. Equation (2–1) applies to the situation where the photosensitizer is an electron donor and transfers an electron to an acceptor (A), and Equation (2–2) applies to the situation where the photosensitizer is an electron acceptor and accepts an electron from a donor (D).

$$\Delta G_0 = E(PS^+/PS) - (E(A/A^-) + E(PS^*)) - \frac{e^2}{\varepsilon}(r_{PS} + + r_{A-}) \quad (2-1)$$

$$\Delta G_0 = (E(PS/PS^-) + E(PS^*)) - E(D^+/D) - \frac{e^2}{\varepsilon}(r_D + + r_{PS-}) \quad (2-2)$$

where E is the relevant reduction potential of the photosensitizer, donor, and acceptor, E(PS*) is the excited-state energy, ε is the dielectric constant of the medium, and r represents the radii of the charge-separated pair.

The terms associated with the photosensitizer in Equations 2–1 and 2–2 can be used to estimate excited-state redox potentials for the photosensitizer. To simplify the abbreviations, from here on we will use the notation $^*E^{ox}$ and $^*E^{red}$ to describe potentials associated with excited-state electron transfer *from* and *to* the photosensitizer, respectively. As shown in Equations 3–1 and 3–2, these potentials are given by the respective ground-state potential, E^{ox} or E^{red}, along with the appropriate excited-state energy. Since the photosensitizers described in this review are all metal-based and operate out of a triplet excited state, we will use the abbreviation "E_{T1}" to describe the triplet-state energy that is needed to calculate excited-state redox potentials.

$$\text{Photoreductant} : *E^{ox} = E^{ox} - E_{T1} \quad (3-1)$$

$$\text{Photooxidant} : *E^{red} = E^{red} + E_{T1} \quad (3-2)$$

Unlike thermal ET, PET is driven by the absorbed photon energy which promotes the ground-state electron to a higher energy level to overcome the activation energy. Thus, ideally, the PET reaction happens only via the bimolecular reaction of the photosensitizer excited state with the donor or acceptor, which is known as dynamic quenching (Figure 1a). While mechanistic studies of catalytic reactions involve many elementary steps beyond

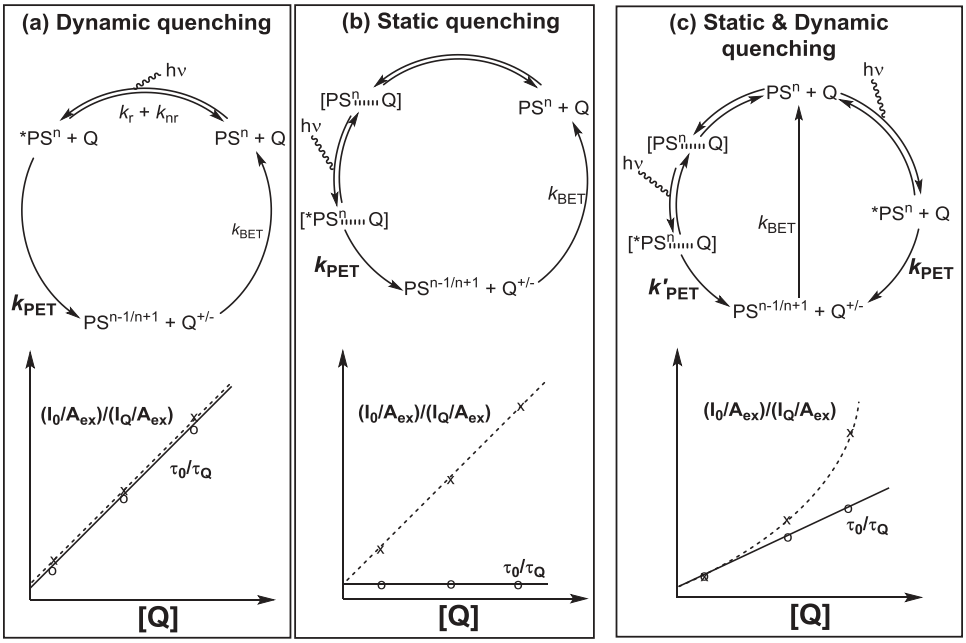

Figure 1. Different types of quenching reaction of the photosensitizer. "PS" is the photosensitizer and "Q" represents the donor or acceptor that is participating in PET with the photosensitizer with an oxidation state (^{n}). Other key abbreviations: *hv* is the photon excitation energy; k_{PET} represents the photoinduced electron transfer rate constant; k_{BET} represents the back-electron transfer rate constant; I_0 and I_Q are the integrated photoluminescence intensity and τ_0 and τ_Q are the photoluminescence lifetimes, in the absence and presence of quencher, respectively; A_{ex} is the absorbance at the excitation wavelength.

electron transfer, the photoluminescence properties of the photosensitizer enable the use of the Stern–Volmer relationship to evaluate electron-transfer kinetics. The Stern–Volmer (S-V) relationship can be evaluated in two ways (bottom of Figure 1a–c): (1) by monitoring the decrease of photoluminescence intensity as quencher (Q) is added ($(I_0/A_{ex})/(I_Q/A_{ex})$); I_0 is the integrated photoluminescence intensity without any quencher present, I_Q is the integrated photoluminescence intensity in the presence of quencher, and A_{ex} is the absorbance at the excitation wavelength); (2) by monitoring the decrease of photoluminescence lifetime (τ_0/τ_Q) after addition of quencher molecule (τ_0 is the native photoluminescence lifetime without any quencher present, τ_Q is the photoluminescence lifetime in the presence of quencher). The combination of these two plots can be used to distinguish the electron-transfer mechanism, as described in Figure 1.[23] In dynamic quenching (Figure 1a), where the photosensitizer excited-state reacts bimolecularly with the quencher, linear and overlaid Stern–Volmer plots are expected. The other extreme is static quenching (Figure 1b), where the ground-state association of the photosensitizer and the quencher precedes PET, and in this situation, the steady-state Stern–Volmer plot follows the normal Stern–

Volmer relationship, whereas the excited-state lifetime (τ) is unaltered. Finally, as shown in Figure 1c it is possible for both mechanisms to occur simultaneously, which results in nonlinear steady-state emission quenching. S-V studies give very limited information about photosensitizer mechanisms, since they are not able to discriminate energy transfer or electron transfer. Thus, to demonstrate electron-transfer quenching it is necessary to directly observe oxidized or reduced photosensitizer and/or quencher molecules via spectroscopic methods such as UV-vis absorption spectroscopy or transient absorption spectroscopy.[24] When the slope (slope = $k_q\tau_0$) of an S-V plot is divided by the native lifetime (τ_0) of photosensitizer, the quenching rate constant (k_q) can be obtained, and when PET is the quenching mechanism this quenching rate constant is equivalent to the electron-transfer rate constant, k_{ET}.

The two major pathways for PET are described in Figure 2. In the first step of Figure 2, photon absorption will generate the PS excited state ($^*PS^n$). For most metal-based photosensitizers, photon absorption is followed by rapid intersystem crossing to a triplet state, on the picosecond timescale for heavy-atom complexes such as *fac*-Ir(ppy)$_3$ (ppy = 2-phenylpyridine).[25] As a result, for such photosensitizers the $^*PS^n$ excited state, from which any potential PET processes occur, is a triplet state. Then, the excited-state complex has three different pathways available in the presence of an electron donor (D) or acceptor (A) molecule. The normal radiative and nonradiative excited-state decay processes, with their associated first-order rate constants k_r and k_{nr}, respectively,

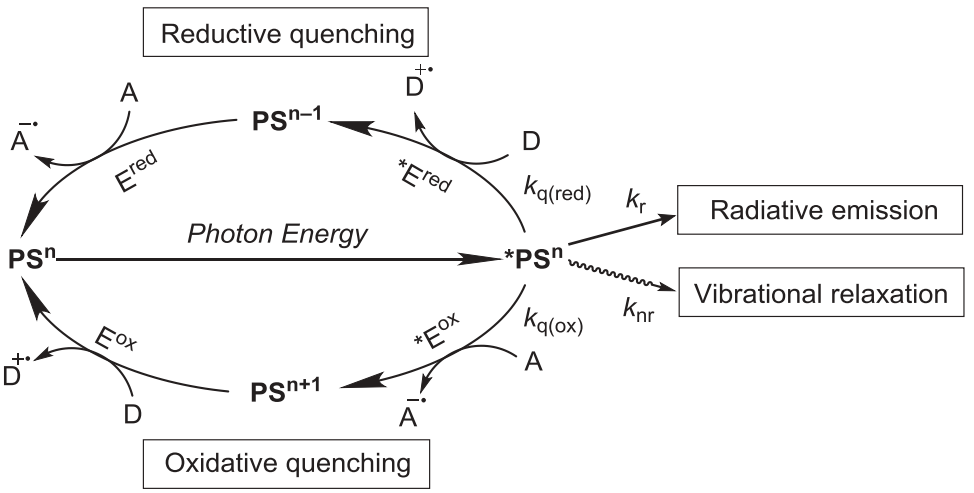

PS^n : *Photosensitizer*, D*: e- donor,* A*: e- acceptor, k_q: quenching rate constant, k_r: radiative rate constant, k_{nr}: non-radiative rate constant*

$^*E^{red} = E(^*PS^n/PS^{n-1})$; $E^{red} = E(PS^n/PS^{n-1})$

$^*E^{ox} = E(PS^{n+1}/^*PS^n)$; $E^{ox} = E(PS^{n+1}/PS^n)$

Figure 2. Electron-transfer pathways for photosensitizers.

compete with the electron-transfer quenching pathways, each with a second-order rate constant k_q. The photosensitizer has two independent electron-transfer pathways following excitation, which are oxidative quenching and reductive quenching. In oxidative quenching electron transfer from the photosensitizer to the quencher occurs, and in reductive quenching electron transfer from the quencher to the photosensitizer occurs. Once a redox reaction happens between the quencher and photosensitizer, in a catalytic reaction the oxidized (PS^{n+1}) or reduced (PS^{n-1}) state of the photosensitizer is required to be reduced or oxidized to its original state by another species, usually a sacrificial redox reagent. In cases of direct activation of the substrate by the photosensitizer, the reducing or oxidizing ability of the photosensitizer can be key factors governing the efficiency of photocatalysis. Thus, understanding both excited-state redox potentials and ground-state redox potentials for the PS is critical.

2.2. *Sensitization-initiated (energy transfer) photocatalysis*

Energy-transfer-initiated photocatalysis is comparably less studied than other electron-transfer-mediated mechanisms. One of the pioneers in this field is the König group.[26] They have shown photocatalysis of halogenated substrates using $[Ru(bpy)_3]^{2+}$ (visible light absorber) and pyrene (triplet energy acceptor). In this mechanism, summarized in Figure 3, the photosensitizer transfers excited-state energy to a triplet acceptor, pyrene. The triplet excited-state of pyrene (Py^{*T1}) is itself very redox active and can undergo reductive quenching with a sacrificial reagent to produce the pyrene radical anion, $Py^{\bullet-}$, which is a strong reductant able to react with organic substrates via single-electron transfer (SET). Another possible fate of the Py^{*T1} is triplet-triplet annihilation, where two equivalents of the triplet combine to form the pyrene singlet state, which itself can participate in redox chemistry.[27,28] $[Ru(bpy)_3]^{2+}$ and pyrene are the first known combination to proceed via sensitization-initiated photocatalysis, but there are decades of research on candidate triplet acceptors beyond pyrene which could be matched with the triplet state of various photosensitizers to expand this photocatalysis mechanism to other systems.[29]

3. Classes of common molecular photosensitizers

3.1. *Ruthenium polypyridyl derivatives*

Having outlined above the function of photosensitizer molecules and considerations of their excited-state and redox chemistry, in this section we will highlight some of the major classes of transition-metal-based photosensitizers and some of their applications in catalysis.

$[Ru(bpy)_3]^{2+}$ (**1**), has the longest history among photoactive late-transition metal complexes with well-defined photophysical properties[16,30] and many

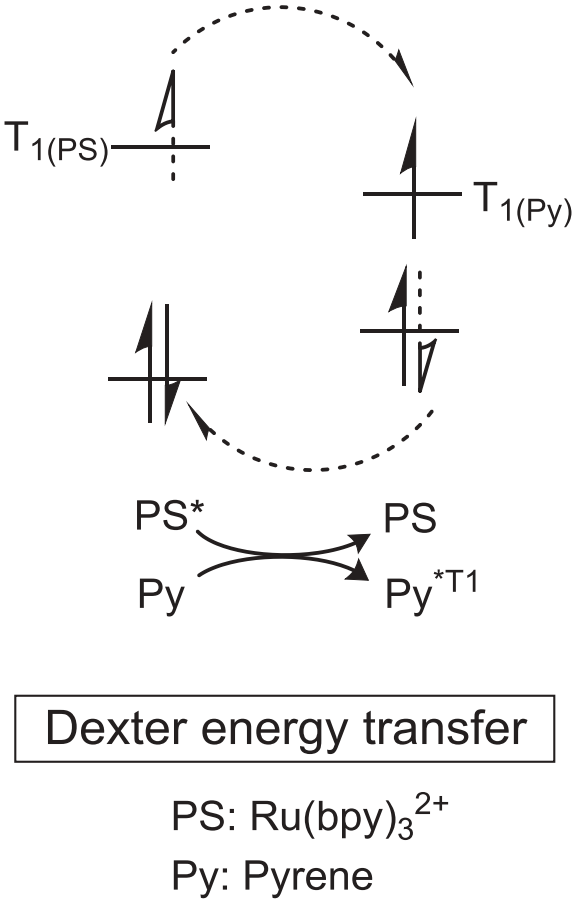

Figure 3. Summary of the sensitization-initiated photocatalytic reaction.

applications in photoredox catalysis.[11] Figure 4 shows the structure of **1** and related ruthenium-based photosensitizers, and Table 1 summarizes their key photophysical and redox properties. Complex **1** has a photoluminescence λ_{max} of 615 nm and its estimated excited-state energy is 2.10 eV. $[Ru(bpy)_3]^{2+}$ (**1**) has lower excited-state reducing power, $E(Ru^{3+}/{}^*Ru^{2+})$ = −1.21 V (reference to vs. $Fc^{+/0}$), compared to other iridium photocatalysts (see below), on account of the Ru complexes having lower HOMO energy levels than the iridium complexes. Nevertheless, **1** has a strong oxidizing ability and a higher reducing power in its reduced ground state following reductive quenching, $E(Ru^{2+}/Ru^{+})$ = −1.73 V, making it a versatile excited-state redox reagent. With this redox ability, several reactions have been introduced such as reduction of electron-deficient olefins, and reductive dehalogenation of various halogenated substrates.[11] It is also possible to halogenate the alcohol functional group in the presence of a halogen source.[15] In the early years of photocatalyst development, several approaches to manipulate the photophysics and redox chemistry of $[Ru(bpy)_3]^{2+}$ (**1**) focused

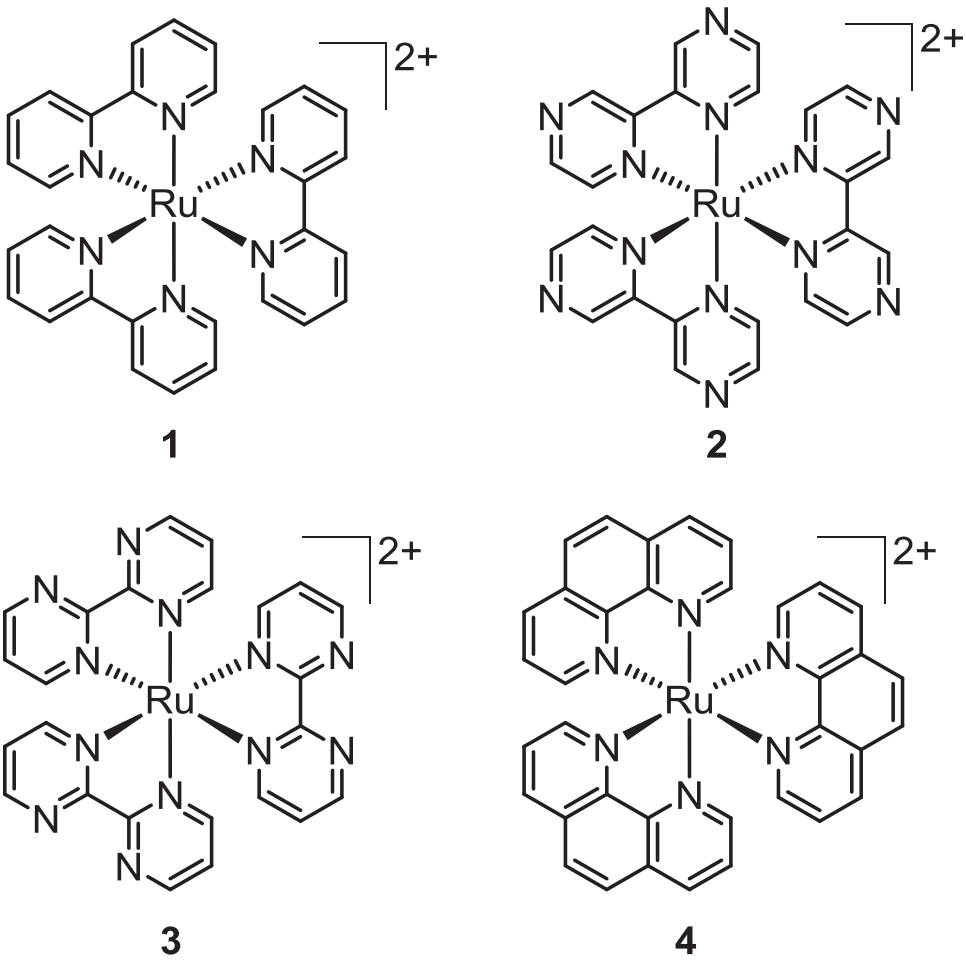

Figure 4. Ruthenium-based photocatalysts.

Table 1. Photoredox properties of complexes **1**–**4**.

	τ (μs)	E_{T1} (eV)	E^{ox} (V)	E^{red} (V)	$*E^{ox}$ (V)	$*E^{red}$ (V)	Ref
1	0.62[a]	2.10	0.89 [a]	−1.73 [a]	−1.21	0.37	[11,13,16,31–34]
2	0.80[b]	2.12	1.46	−1.20	−0.66	1.85	[13,17,35]
3	0.13[b]	1.90	1.29	−1.39	−0.61	0.59	[30,35]
4	0.92[a]	2.15	0.86	−1.76	−1.27	0.42	[35]

*All redox and excited-state redox potential were corrected from reported experimental condition vs. $Fc^{+/0}$ according to the following conversions[36]: ($Fc^{+/0}$ = 0.40 V vs SCE (MeCN/[NBu_4][PF_6]). $Fc^{+/0}$ = 0.45 vs SCE (DMF/[NBu_4][ClO_4]. $Fc^{+/0}$ = 0.45 V vs SCE (DMF/[NBu_4][PF_6]). $Fc^{+/0}$ = 0.40 V vs NHE in H_2O. $Fc^{+/0}$ = 0.51 V vs SCE (glyme/[NBu_4][PF_6]). $Fc^{+/0}$ = 0.46 V vs SCE (CH_2Cl_2/[NBu_4][PF_6]). $Fc^{+/0}$ = 0.56 V vs SCE (THF/[NBu_4][PF_6]). $Fc^{+/0}$ = 0.43 V vs SCE (DMSO/[NBu_4][PF_6]). $Fc^{+/0}$ = 0.31 V vs SCE (MeCN/Na[ClO_4])).

[a]RT in H_2O.

[b]RT in polycarbonate.

on modifications to the bipyridyl ligand. $[Ru(bpz)_3]^{2+}$ (bpz = 2,2′-bipyrazine) (**2**) and $[Ru(bpm)_3]^{2+}$ (bpm = 2,2′-bipyrimidine) (**3**) are simply modified by adding nitrogen atoms to the bipyridine ligand, which inductively withdraw electron

density. While they have relatively unchanged photophysical properties, their HOMO and LUMO energy levels are quite different, as discerned by redox potentials that are cathodically shifted by 400 to 600 mV compared to complex **1**. These trends demonstrate that the electron-deficient bpz and bpm ligands stabilize both the HOMO and LUMO energy levels.[30] Complexes **2** and **3** have found utility in certain photoredox transformations, including dehalogenation reactions, photocatalytic thiol-ene addition, and cycloaddition.[37,38] $[Ru(phen)_3]^{2+}$ (phen = 1,10-phenanthroline) (**4**) is less known for its photocatalytic activity compared to **1** and has similar photophysical and electrochemical characteristics except for different k_r and k_{nr} values which lead to a higher photoluminescence quantum yield (Φ_{PL}) and longer lifetime (τ). A recent report from Han and Cho supports that **4** is catalytically active, promoting the trifluoromethylation of alkenes with better *E: Z* selectivity than **1**.[39,40]

3.2. *Cyclometalated iridium complexes*

3.2.1. *Homoleptic iridium complexes*

Homoleptic tris-cyclometalated iridium complexes are typically more photostable and photoreducing than ruthenium polypyridyl photosensitizers. As a result, in recent years an increasing proportion of photoredox methodological developments involves iridium-based photosensitizers. Pioneers in this field include the groups of Macmillan[12,46,49–51] and Stephenson.[15,34,43,52–54] The structures of homoleptic iridium complexes are drawn in Figure 5 and their properties are listed in Table 2. The complex *fac*-$Ir(ppy)_3$ (**5**) is one of the strongest photoreductants commonly used in photoredox catalysis, and has well-established photophysical and electrochemical properties.[2,55,56] The excited-state energy (2.51 eV) and the ground-state redox potentials ($E(Ir^{IV/III})$ = 0.38 V and $E(Ir^{III/II})$ = −2.60 V), which are the two components of the excited-state potentials, result in the excited state of **5** being ~900 mV more reducing but ~500 mV less oxidizing than $[Ru(bpy)_3]^{2+}$ (**1**). Complex **5** also has a longer lifetime than **1**, which contributes to the efficient PET that is essential for photocatalysis. With the high reducing ability, **5** is particularly adept at reducing halogenated substrates via hydrodehalogenation, capable of activating all of C–I[43], C–Br[21], C–Cl[57], and C–F[58] bonds. The expansion of the tris-cyclometalated iridium complex library is accomplished by introducing electron-withdrawing groups (F, CF_3) or electron-donating groups (CH_3, t-Butyl or OMe) onto the 2-phenylpyridine cyclometalating ligand. Complexes **6**–**8** show the effects of electron-deficient functional groups with anodically shifted first redox potentials and variations in the excited-state energy from 2.22 to 2.90 eV.

Nacsa and Macmillan have modified *fac*-$Ir(ppy)_3$ with *tert*-butyl groups or methoxy groups **9**–**16**,[46] with some of these complexes reported earlier by Watts.[41] The photophysical properties of these variants were not studied in

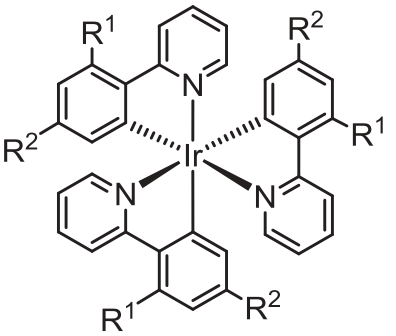

5: R^1= H, R^2=H
6: R^1= F, R^2=F
7: R^1= H, R^2=F
8: R^1= H, R^2=CF_3

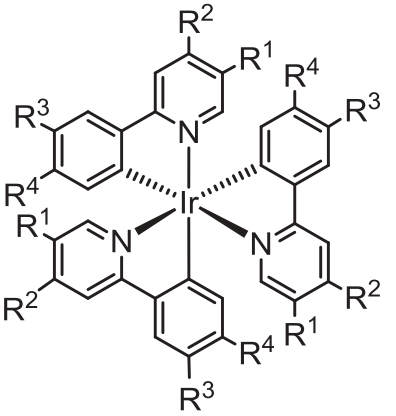

9: R^1= tBu, R^2,R^3,R^4 = H
10:R^2= tBu, R^1,R^3,R^4 = H
11: R^3= tBu, R^1,R^2,R^4 = H
12: R^4= tBu, R^1,R^2,R^3 = H
13: R^2= OMe, R^1,R^3,R^4 = H
14: R^3= OMe, R^1,R^2,R^4 = H
15: R^4= OMe, R^1,R^2,R^3 = H
16: R^2,R^3,R^4= OMe, R^1 = H
17: R^3= SO_3^-, R^1,R^2,R^4 = H

Figure 5. Homoleptic iridium complexes.

Table 2. Photoredox properties of complexes **5**–**17**.

	τ (μs)	E_{T1} (eV)	E^{ox} (V)	E^{red} (V)	$*E^{ox}$ (V)	$*E^{red}$ (V)	Ref
5[a]	1.9	2.51	0.38	−2.60	−2.13	−0.09	[33,41–43]
6[b]	1.57	2.22	0.54	−2.27	−1.68	−0.04	[42,44]
7[a]	2.04	2.77	0.46	−2.58	−2.31	0.29	[41]
8[a]	2.16	2.90	0.81	−1.61	−2.09	0.19	[41,45]
9[a]	n/a	2.58	0.37	−2.70	−2.21	−0.12	[46]
10[c]	n/a	2.58	0.22	n/a	−2.40	n/a	[46]
11[a]	n/a	2.52	0.28	−2.66	−2.24	−0.14	[46]
12[a]	1.97	2.56	0.26	−2.73	−2.30	−0.17	[41,46]
13[c]	n/a	2.59	0.13	n/a	−2.46	n/a	[46]
14[a]	2.86	2.40	0.19	−2.61	−2.21	−0.21	[41,46]
15[a]	2.24	2.64	0.36	−2.74	−2.29	−0.14	[41,46]
16[a]	n/a	2.42	−0.12	n/a	−2.53	n/a	[46]
17[d]	1.6	2.65	0.36	n/a	−2.29	n/a	[47,48]

[a]Redox potentials in MeCN.
[b]Conditions unknown.
[c]Redox potentials in CH_2Cl_2.
[d]Redox potentials in H_2O.
n/a, not reported.

great detail, but their electrochemical properties and calculated excited-state redox potentials fall in a narrow range. Thus, in surveying the whole set of iridium homoleptic complexes **5**–**16**, it appears that electron-withdrawing

functional groups such as F or CF_3 groups are more effective at perturbing the relevant energy levels of the iridium complex.

One other reported modification to homoleptic tris-cyclometalated iridium complexes is the incorporation of water-solubilizing sulfate groups, in complex **17**. Wenger has disclosed the synthesis of **17** and its photocatalytic application in the hydrogenation of pyrroline derivatives with better yields than **5**.[47] Also, they have shown the strong reducing ability of **17** with activation of activated alkyl chloride and alkyl fluoride substrates, and degradation of ammonium substrates.[48]

3.2.2. *Heteroleptic iridium complexes*

In addition to homoleptic tris-cyclometalated iridium complexes, heteroleptic bis-cyclometalated analogues have become prominent as photosensitizers. These heteroleptic complexes offer many potential advantages over their homoleptic analogues. The ancillary ligand(s) give additional layers of control over the molecular and electronic structure, and often impart greater solubility when compared to homoleptic tris-cyclometalated complexes. Most heteroleptic iridium complexes are prepared from chloride-bridged iridium dimers of the type $[Ir(C\hat{}N)_2(\mu\text{-}Cl)]_2$ (C^N = cyclometalating ligand), which are accessed under simple reaction conditions from $IrCl_3$ and the cyclometalating ligand. In such heteroleptic structures, cationic complexes with bipyridine-derived ancillary ligands are widely investigated. Bernhard and coworkers have developed various cationic cyclometalated iridium complexes with modified bipyridine ancillary ligands for photocatalytic H_2 generation.[60,62,70] There are examples of heteroleptic iridium complexes in Figure 6 and 7, and their properties are summarized in Table 3. Among them, most well-established structures are $[Ir(ppy)_2(dtbbpy)]^+$ (ppy = 2-phenylpyridine, dtbbpy = 4,4′-di-tert-butyl-2,2′-bipyridine) (**18**) and $[Ir(dF(CF_3)ppy)_2(dtbbpy)]^+$ (dF(CF_3)ppy = 2-(2,4-difluorophenyl)-5-(trifluoromethyl)pyridine) (**19**). Replacement of one 2-phenylpyridine ligand with a π-accepting bipyridine ligand greatly stabilizes the energy levels of both the HOMO and LUMO. In computational studies of $[Ir(C\hat{}N)_2(bpy)]^+$ complexes, the majority of electron density at the HOMO energy level comes from the iridium metal center and the C^N ligands, whereas electron-density in the LUMO is primarily localized on the bpy ligand. Thus, modification of the C^N ligands with electron-withdrawing group changes the HOMO energy level while minimally impacting the LUMO energy level in complex **19**.[62]

Another example of an iridium photosensitizer with a modified bipyridine ligand is $[Ir(ppy)_2(ptdtb)]^+$ (ptdtb = N,N'-1,10-phenanthrolinedithiino[2,3-*b*] benzene) (**20**). Erdmann et al. have introduced this N^N ancillary ligand related to phenanthroline but with a dithio linker to extend the conjugation off of the central arene ring. Enlarging the aromatic ring resulted in a significant increase of the excited-state lifetime to 47 μs.[64] Whang et al.

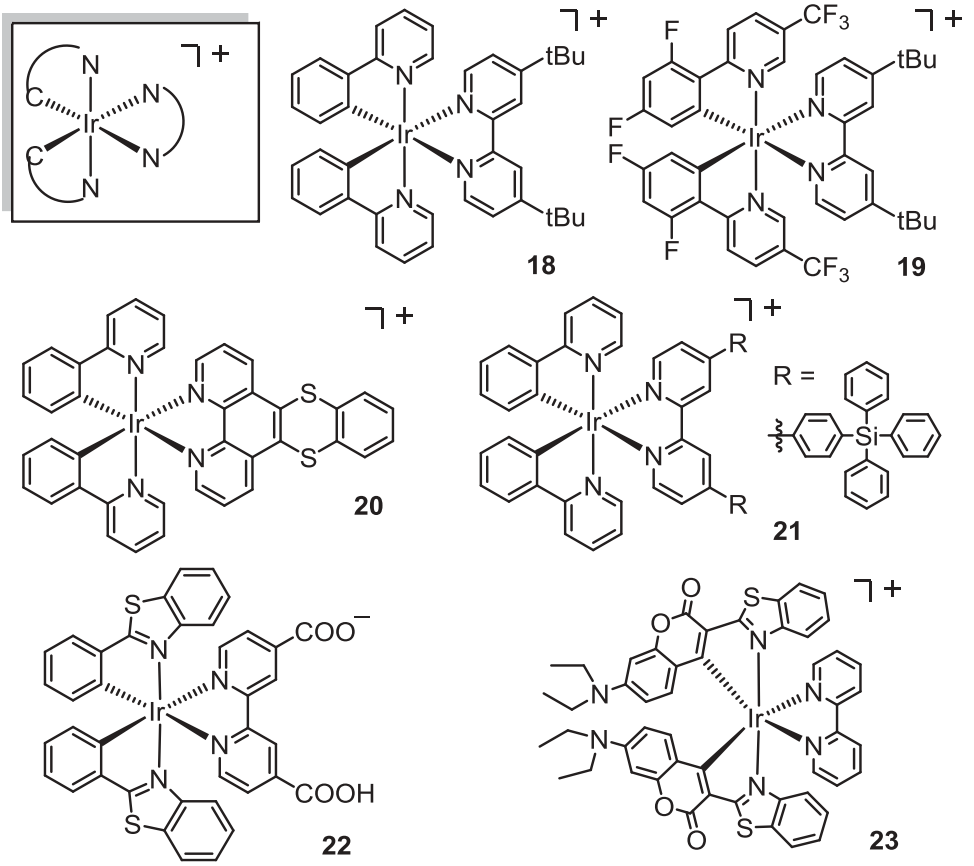

Figure 6. Iridium-based photocatalysts with N^N type ancillary ligand.

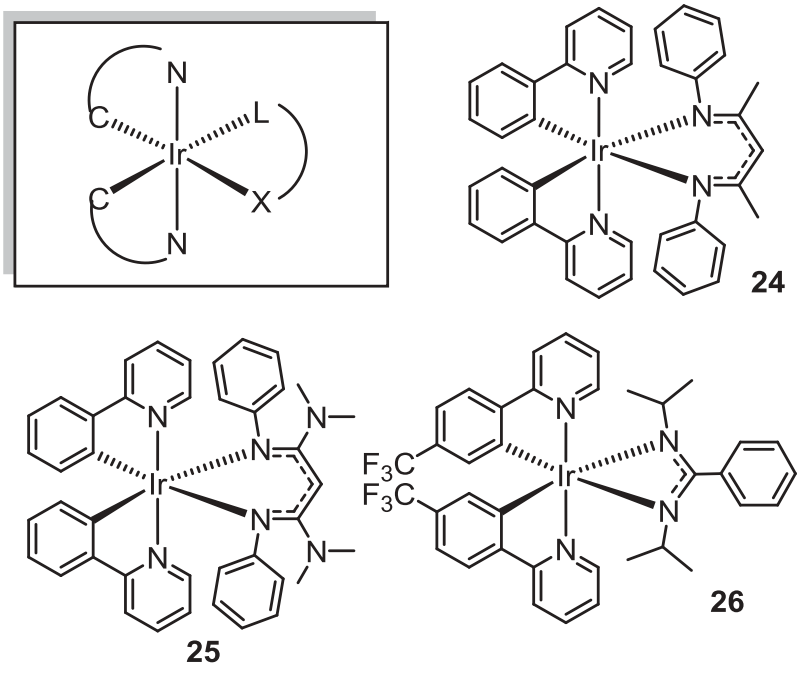

Figure 7. Iridium-based photocatalysts with L^X type ancillary ligand.

Table 3. Photoredox properties of complexes **18**–**28**.

	τ (μs)	E_{T1} (eV)	E^{ox} (V)	E^{red} (V)	$*E^{ox}$ (V)	$*E^{red}$ (V)	Ref
18[a]	0.60	2.17	0.81	−1.61	−1.36	0.26	[33,54,59_63]
19[a]	2.3	2.58	1.29	−1.77	−1.61	0.49	[12,33,62]
20[a]	47.1	2.13	0.91	−1.69	−1.22	0.52	[64]
21[b]	0.47	2.34	0.71	−1.66	−1.63	0.71	[65]
22[b]	0.099	2.38	0.80	−1.46	−1.58	0.80	[6]
23[a]	0.081	2.13	0.70	−1.60	−1.43	0.53	[66]
24[a]	0.20	2.4	−0.07	−2.4	−2.5	0.0	[20,21]
25[a]	0.76	2.3	−0.26	−2.7	−2.6	−0.4	[20,21]
26[c]	0.069	2.33	0.26	−2.29	−2.07	0.04	[67]
27[a]	0.55	n/a	0.84	−1.81	n/a	n/a	[68]
28[a]	2.6	n/a	1.33	−1.44	n/a	n/a	[69]

[a]In MeCN.
[b]In THF
[c]In CH_2Cl_2.
n/a, not reported.

used tetraphenylsilane functional groups to modify various positions on the $[Ir(ppy)_2(bpy)]^+$ complex. A significant increase of turnover the number for photocatalytic hydrogen gas evolution was obtained with the complex $[Ir(ppy)_2(4,4'$-(ditetraphenylsilane)-bpy$)]^+$ (**21**).[65] Further modification of iridium complexes with alternative cyclometalating ligands derived from coumarin, introduced by Takizawa et al., resulted in complexes with strongly solvent-dependent lifetimes. The lifetime of **23** is 8.5 μs in CH_2Cl_2 and it drops to 81 ns in acetonitrile. And methylation on 4-position of the bpy ligand yields highly increased lifetime up to 23 μs in CH_2Cl_2.

Commonly, neutral heteroleptic $Ir(C\hat{}N)_2(L\hat{}X)$ complexes can be prepared from the reaction of 2 equivalents of the ancillary ligand and 1 equivalent of the bis-cyclometalated iridium chloride-bridged dimer. To manipulate the HOMO energy level of the iridium chromophore, π-donating ancillary ligands can be used in the heteroleptic complexes. Our group has investigated the effects of modified β-diketiminate (NacNac) ligands on bis-cyclometalated iridium complexes. Figure 7 shows the structures of **24** and **25**, two of the best-studied β-diketiminate complexes, and many other substituted variants have been investigated as well.[20,21] The results show that the HOMO energy level, which is related to the first oxidation potential (E^{ox}), varies from +0.03 V to −0.39 V depending on the substitution of the NacNac. Even though the significant destabilization of the HOMO energy also decreases the excited-state energy (E_{T1}), the overall excited-state oxidation potential ($*E^{ox}$) has been cathodically shifted to values as negative as −2.6 V.[20,71] These strongly reducing photosensitizers enable the photocatalytic hydrodebromination of aryl bromide substrates under very simple conditions, without any silane radical mediators as additives.

Amidinate (R′NC(R)NR′) ligands are commonly used for various transition-metal complexes, particularly in chemical vapor deposition precursor

compounds.[72] Liu et al. have reported a phosphorescent amidinate-ligated iridium bis(2-phenylpyridine) complex[73], and Yu et al. have documented the photocatalytic activity of a modified iridium amidinate complex, $Ir(tfm\text{-}ppy)_2(dipba)$ (tfm-ppy = 2-[4-(trifluoromethyl)phenyl]-pyridine), dipba = *N,N′*-diisopropylbenzamidinate) (**26**) for water reduction.[67] In this photocatalytic study, they modified the phenyl group on the backbone of the amidinate with an electron-donating group. The photophysical and electrochemical properties of the modified complex are minimally changed. However, the photocatalytic activities of two amidinate complexes are higher than a charged complex, $[Ir(tfm\text{-}ppy)_2(dtbbpy)]^+$ (dtbbpy = 4,4′-ditert-butyl-2,2′-bipyridyl).

3.2.3. *Iridium pincer complexes*

Many iridium pincer complexes have been developed for the purpose of dehydrogenation and related reactions, using PCP and NCN type pincer ligands.[74] The Pincer iridium complexes are described in in Figure 8 and Table 3. After the emissive iridium pincer complexes[75,76] were reported, Tinker and Bernhard demonstrated a photocatalytic system for hydrogen gas evolution using the homoleptic iridium pincer complex $[Ir(phbpy)_2]^+$ (**27**, phbpy = 6-phenyl-2,2′-bipyridine). They have shown improved robustness of the iridium complex in the photocatalytic reaction, and a TON two times larger than bidentate iridium complexes such as $[Ir(ppy)_2(bpy)]^+$.[68] In addition, Sato et al. have reported photocatalytic carbon dioxide reduction reaction with $[Ir(tpy)(ppy)Cl]^+$ (**28**, tpy = terpyridine).[69]

3.3. *Pt complexes*

Platinum-based organometallic complexes are less studied as photosensitizers than their ruthenium and iridium counterparts, but there are examples of organoplatinum complexes in photocatalytic applications, which are shown in

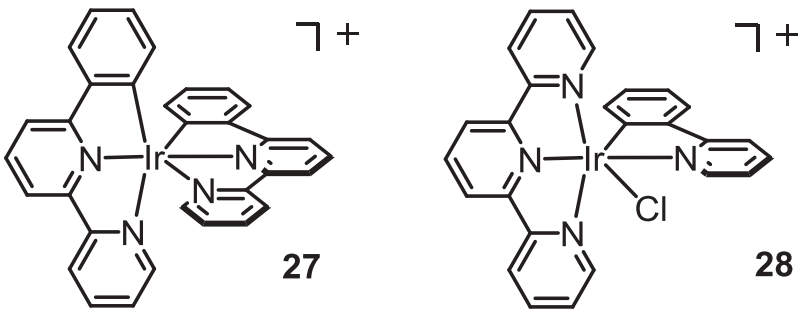

Figure 8. Iridium-based photocatalysts with pincer ligands.

Figure 9 and Table 4. Yang et al. have followed up on earlier reported platinum terpyridyl acetylide complexes of Yam et al.[82], preparing highly emissive complex **29** which Du et al. applied in the photocatalytic hydrogen evolution reaction.[77,83] Complex **29** has low-energy visible absorption between 375 and 540 nm and emits photoluminescence with λ_{max} at 605 nm. Diacetylide platinum complex **30** has well-characterized electrochemical and excited-state properties, as reported by Castellano and coworkers, with isolated reports on the photocatalytic performance.[79] Several other substituted analogues of **30** have also been described by Eisenberg and several others.[84] A later study of modified Pt pincer complexes also characterized their photocatalytic performance in hydrogen evolution reaction.[85] Photocatalytic trifluoromethylation of alkenes and heterocycles using the cyclometalated Pt complexes Pt(C^N)(acac) (C^N = 2-phenylpyridine, (**31**) 2-(2,4-difluorophenyl)pyridine (**32**), and 2-(3-methoxyphenyl)pyridine (**33**), acac = acetylacetonate) and its mechanistic studies were reported by Choi et al.[80] Complex **34** is one of the many well-characterized structures by De Cola and coworkers. It has relatively high photoluminescence quantum yield (73%) and a longer lifetime (14.59 μs) than most platinum-based organometallic complexes.

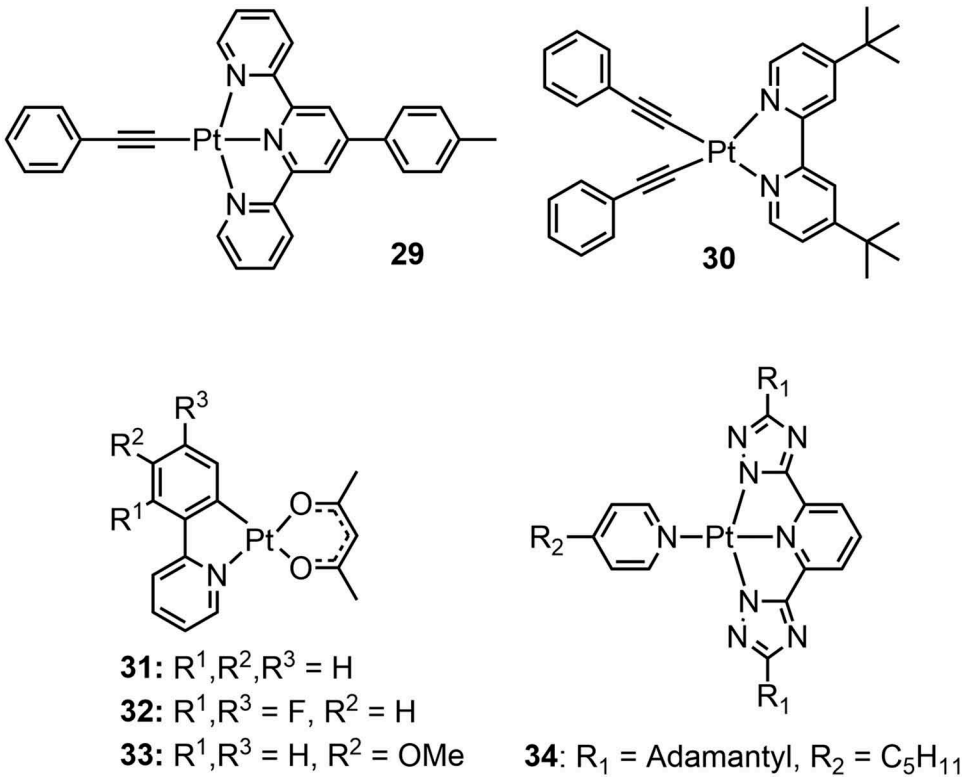

Figure 9. Platinum-based photocatalysts.

Table 4. Photoredox properties of complexes **29**–**34**.

	τ (μs)	E_{T1} (eV)	E^{ox} (V)	E^{red} (V)	$*E^{ox}$ (V)	$*E^{red}$ (V)	Ref
29[a]	4.6	2.46	0.65	−1.28	−1.81	1.18	[77,78]
30	2.56	2.49	n/a	−1.77	n/a	0.72	[79]
31[b]	2.2	2.64	0.17	−2.78	−2.47	−0.14	[80]
32	0.382	2.73	0.22	−2.86	−2.51	−0.13	[80]
33	11.6	2.45	0.12	−2.60	−2.33	−0.15	[80]
34	14.14	2.51[c]	1.05	−2.10	−1.46	0.41	[81]

[a]in CH_2Cl_2.
[b]In MeCN .
[c]Calculated from emission at 77 K.
n/a, Not reported.

3.4. *Other metal complexes*

Other transition metals beyond iridium and ruthenium also have the potential to be developed as alternative photosensitizers, with relatively undiscovered photophysical properties. The structures of these complexes are in Figure 10 with their properties summarized in Table 5. The first zirconium-based photosensitizer has been reported by the Milsmann group with two redox-active pincer ligands. They have utilized the green LED light source for their photoreaction since the absorption band of **35** is around 550 nm. Under the reductive quenching mechanism, benzyl bromide is successfully converted to bibenzyl with benzimidazolium hydride as a sacrificial reagent.[86] Group 6 isocyanide complexes have also recently emerged as versatile photosensitizers, including chelated Mo complex (**36**) by Büldt, Wenger *et al.*[87] and monodentate, homoleptic W complexes (**37**) by Sattler, Gray *et al.*[88] as representative examples. Both have cathodically shifted oxidation potentials compared to other complexes which permit high excited-state reducing power ($*E^{ox}$), namely −2.6 V for **36** and −3.0 V for **37**. The catalytic potential of **36** was demonstrated by the photocatalytic rearrangement of an acyl cyclopropane to a 2,3-dihydrofuran, which occurs with visible light irradiation (λ = 455 nm) and a TON of 17.

Pirtsch *et al.* have used a copper-based photosensitizer, $[Cu(dap)_2Cl]$ (dap = 2,9-bis(para-anisyl)-1,10-phenanthroline) (**38**), to perform the photocatalytic reaction of atom-transfer radical addition or allylation.[90] In addition to copper complex **38**, the potential of first-row transition metal complexes (Cu, Zn, Ni) to serve as photosensitizers is summarized by Hockin *et al.*[94] Iron complexes are ideal candidates for future photoredox chemistry, given the large natural abundance of this metal. One major drawback of iron complexes as photosensitizer is that they typically have sub-nanosecond lifetimes, e.g. τ ($[Fe(bpy)_3]^{2+}$) <1 ns. The short excited-state lifetime is due to low-lying, metal-centered (^{3}MC) states positioned between the metal-to-ligand charge transfer (^{3}MLCT) state and the ground state (S_0), which leads to fast, nonradiative vibronic relaxation. Recent studies are

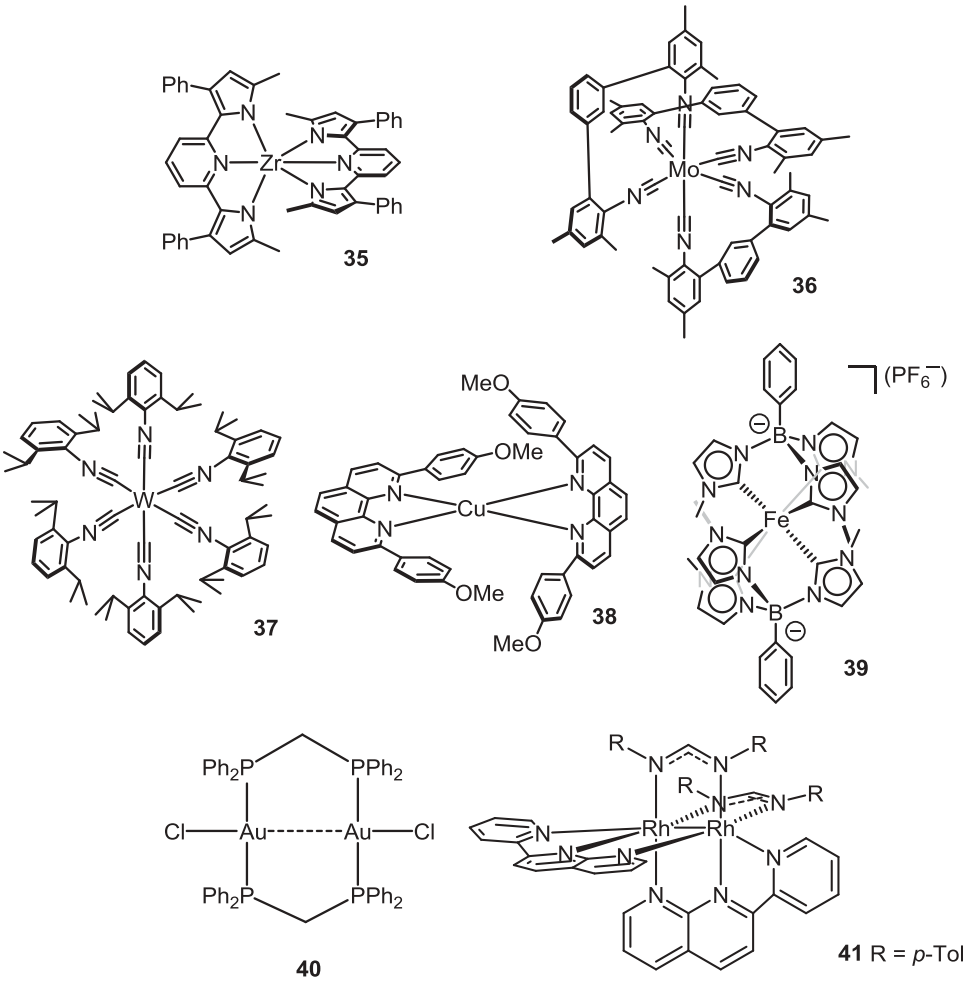

Figure 10. Other metal-based photocatalysts.

Table 5. Photoredox properties of complexes **35**–**41**.

	τ (μs)	E_{T1} (eV)	E^{ox} (V)	E^{red} (V)	$*E^{ox}$ (V)	$*E^{red}$ (V)	Ref
35[a]	325	2.09	n/a	−2.16	n/a	−0.07	[86]
36	b	2.2	−0.40	n/a	−2.6	n/a	[87]
37[c]	0.075	2.28	−0.72	n/a	−3.00	n/a	[88]
38[d]	0.27	2.05	0.22	n/a	−1.83	n/a	[89,90]
39[e]	0.002	2.13	0.23	−1.13	−1.9	1.0	[91]
40[d]	1.56	3.5	0.2	−3.3	−2.0	1.5	[92]
41	0.012	1.3	0.52	−1.10	−0.78	0.20	[93]

[a]In THF.
[b]Bi-exponential 6.4 μs (48%), 27.9 (52%) at 77 K.
[c]Toluene.
[d]CH_2Cl_2.
[e]In MeCN.

focusing on the manipulation of the excited-state energy levels via ligand modification.[95] A significant breakthrough was realized with the iron(III) complex $[Fe(phtmeimb)_2]^+$ (**39**, phtmeimb = phenyl(tris(3-methylimidazol-1-ylidene))borate), which has a 2-ns excited-state lifetime at room temperature.[91] The dinuclear gold complex (**40**) is another noble metal-based photosensitizer that has been explored recently, one drawback being it does not absorb in the visible region and can only be excited in the UV, with absorption bands at 258 nm and 320 nm. With UV excitation, **40** can be used for the photocatalytic atom transfer radical polymerization (ATRP) of (meth) acrylates.[92] In the recent work of Whittemore et al. on the dirhodium complexes **41**, they were able to observe excited-state charge transfer between an electron donor (*p*-phenylenediamine) and the dirhodium complex to estimate the electron transfer rate. This result supports that complex **41** is also a strong candidate for photoredox catalysis even though it has a relatively short excited-state lifetime of 12 ns.

4. Examples of organic synthesis via photoredox catalysis

The above sections of this review summarized the principles of metal-based photosensitizers, and gave numerous examples of photosensitizers that have become prominent in the recent literature. Although the major focus of this review is structure–property relationships in metal-based photosensitizers, in this closing section we do want to provide specific examples of applications of these complexes in catalysis. Acknowledging there are many other important photocatalytic reactions in the literature beyond what we discuss here, in this section, we highlight a select few reductive transformations initiated by outer-sphere excited-state electron transfer, showing a diverse range of transformations that can be carried out with a metal-based photosensitizer.

4.1. *Small molecule activation*

4.1.1. *Reactions of organohalide substrates*

Figure 11 summarizes several advances in photoredox reactions of alkyl and aryl halide substrates.[12,43,49–52,54,63] Included in these results are simple dehalogenation reactions, functional group transformations where the organic radical is trapped by a second reagent, as well as radical cyclization reactions initiated by dehalogenation. Iridium-based photosensitizers are most prominent, especially for reactions involving relatively unactivated substrates, and a number of sacrificial reagents and additives have been used to promote these reactions.

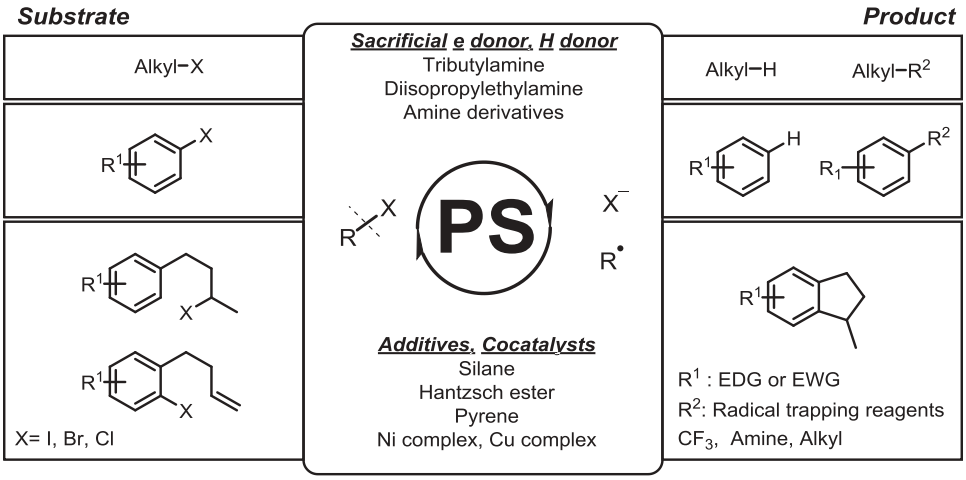

Figure 11. Photocatalytic dehalogenation reaction of alkyl- or aryl-halogenated substrate.

4.1.2. *Photocatalytic organic synthesis with non-halogenated substrates*

Although halogenated substrates summarized above are particularly prominent in photoredox catalysis, photoredox reactions with other substrates are becoming more and more common. Examples include C–C bond cleavage[96], C–H functionalization[97,98], oxidative cyclization[38,99], alkene reduction[100], cycloaddition[14,101,102], and trifluoromethylation.[31,39,49] Organometallic photosensitizers are likewise prominent in these synthetic applications, which highlight the growing diversity of photoredox catalysis as a synthetic strategy.

4.1.3. *Photocatalytic hydrogen gas evolution from water*

A large number of research groups have contributed to the field of photocatalytic hydrogen evolution, using water or mineral acids as the precursor.[60,65,67,103–112] This work is motivated by the need to discover practical and efficient means of storing solar energy, with water splitting being one of the most promising solutions. Photocatalytic hydrogen evolution schemes have used both organic and metal-based photosensitizers, and typically the reaction system is either two-component (photosensitizer and catalyst) or three-component (photosensitizer, electron relay (ER), and catalyst), as summarized in Figure 12. Both oxidative and reductive quenching pathways can be operative in photocatalytic hydrogen evolution, and a variety of photosensitizers and catalysts have found success in this area.

4.1.4. *Photocatalytic reduction of carbon dioxide*

In addition to proton reduction to hydrogen, many photocatalytic systems have been developed for CO_2 reduction, to CO or other reduced products.[113–119] Figure 13 summarizes two representative examples of CO_2 reduction

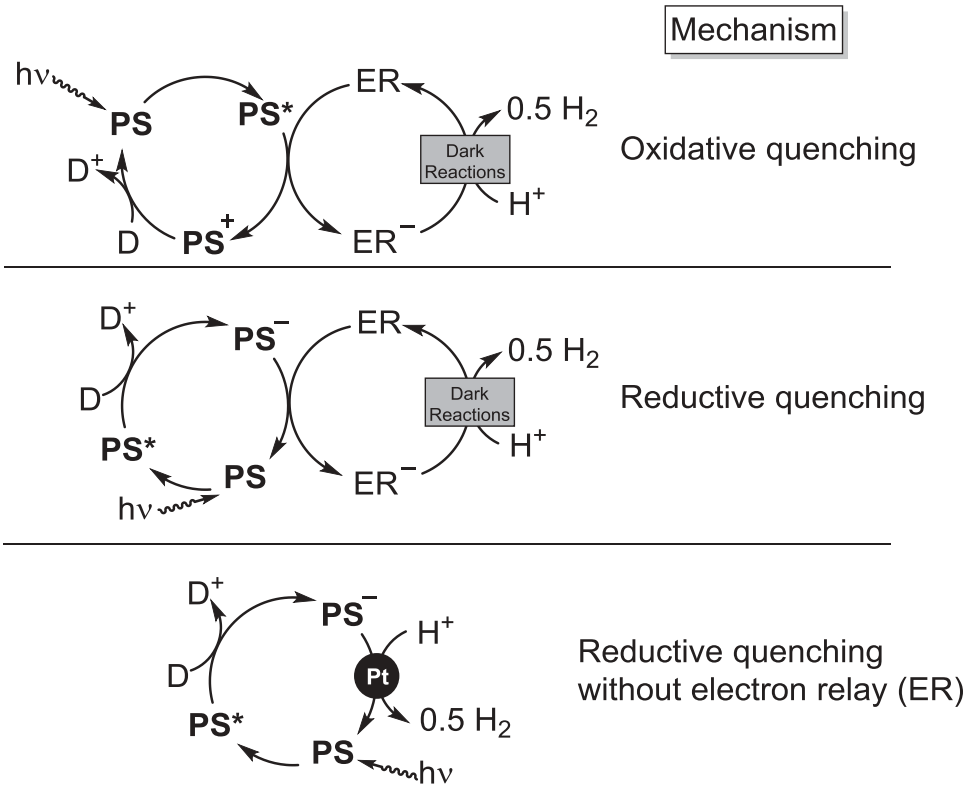

Figure 12. Mechanisms in photocatalytic hydrogen gas evolution, based on work from Tinker et al.[111]

photocatalysis, highlighting two different approaches. In the top panel of Figure 13, work from Sato et al. is summarized, in which photocatalytic CO_2 reduction is carried out *without* cocatalyst. In this system, iridium complex **28** serves as both the light absorber and the catalyst, reducing CO_2 with triethanolamine (TEOA) as a sacrificial reductant. The bottom panel of Figure 13 summarizes work from Robert, Lau, et al., where homoleptic iridium photosensitizer **5** is used in concert with a cobalt CO_2 reduction catalyst. In this system, the proposal is that complex **5** is oxidatively quenched by the cobalt precatalyst following visible-light excitation, and a second oxidative quenching event further reduces the catalyst prior to CO_2 activation. Triethylamine was used as a sacrificial reductant, and turnover numbers as high as 270 were achieved.

4.1.5. *Lignin degradation via carbon-oxygen bond cleavage*

Recent work has also revealed photoredox catalysis to be a promising means of degrading lignin biomass, in the context of preparing fuels and commodity chemicals from renewable biomass sources.[53,61,120–123] In the photochemical degradation of lignin model compounds, described in Figure 14, the native benzyl alcohol functional group of the lignin β-O-4 linkage is first oxidized to

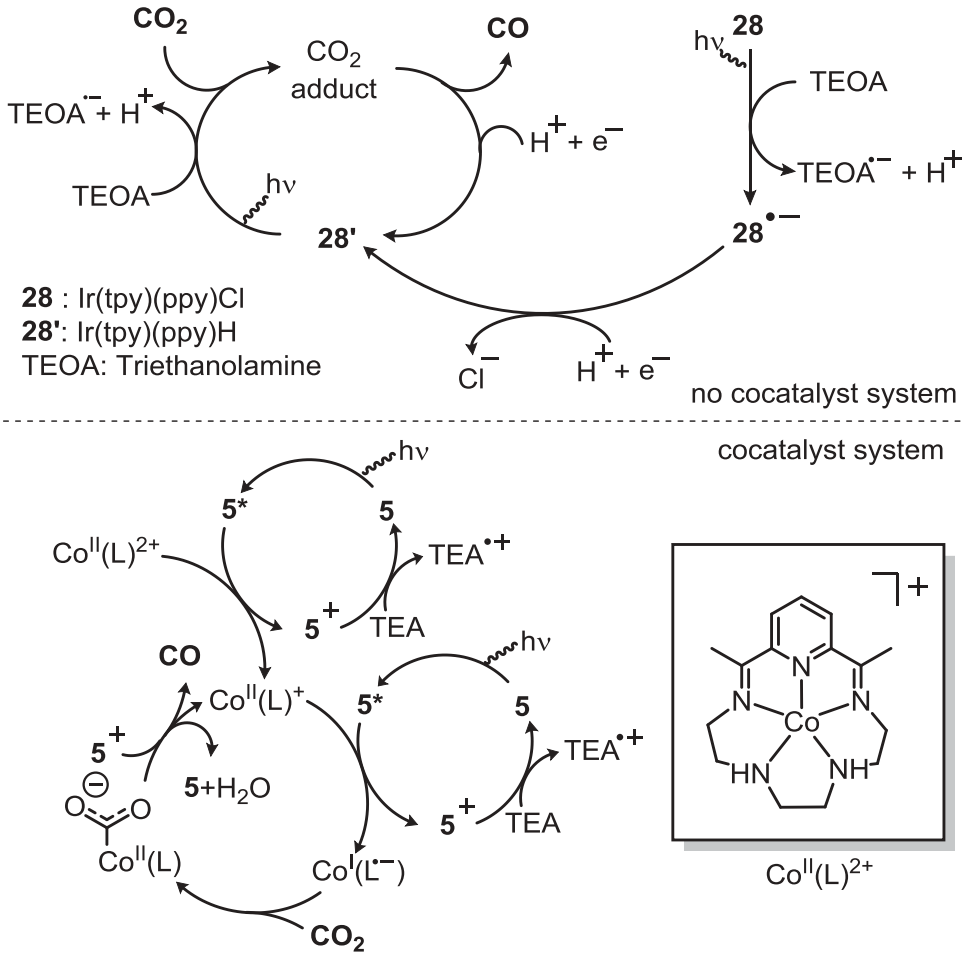

Figure 13. Photocatalytic reduction of carbon dioxide molecule, originally reported by Sato et al.[69] and Chen et al.[117]

a carbonyl, which sufficiently weakens the neighboring ether C–O bond to allow photoactivation. Photoredox cleavage of lignin models is accomplished with reducing iridium photosensitizers such as **5** and **18**, using tertiary amines as sacrificial reductants.

4.1.6. *Photoredox polymer synthesis*

In addition to small-molecule organic chemistry and solar fuels described above, photoredox catalysis has also emerged in macromolecular science. Most commonly, strongly photoreducing complexes are used to initiate radical polymerization via carbon-heteroatom bond activation, with a few different approaches emerging recently. As shown in Figure 15a, one approach uses a single-component photocatalyst where a bis(1,10-phenanthroline)copper(I) complex

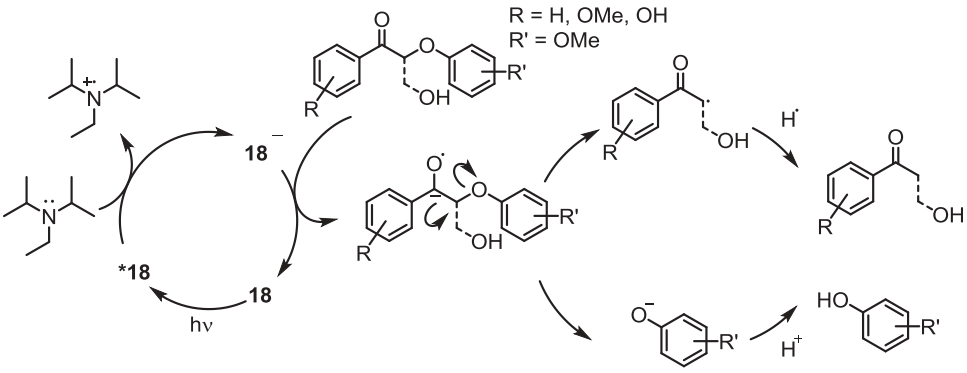

Figure 14. Photocatalytic reductive cleavage of oxidized lignin model systems.[121].

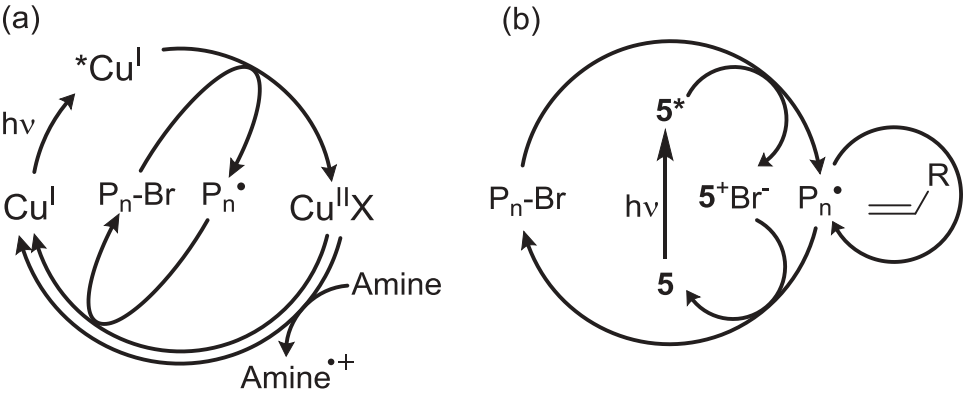

Figure 15. (a) Photocatalytic atom transfer radical polymerization (ATRP) with Copper photosensitizer (Cu^{I} = bis(1,10-phenanthroline)copper(I)), originally reported in reference [124] (b) Proposed mechanism of photocatalytic living radical polymerization with the complex **5**. P_n = polymer chain, M = monomer. Scheme based on work Fors et al.[125]

serves as both light absorber and catalyst, promoting radical chain growth via photochemical C–Br bond activation.[124] A second approach, in which visible light is used to control radical polymerization of methacrylates, is shown in Figure 15b.[125] Here, iridium photosensitizer **5** was used, and following visible-light excitation it was oxidatively quenched by the initiator ethyl-α-bromophenylacetate, generating a radical which then reacts with methacrylate monomer to kick off radical polymerization. The light input afforded excellent control over polymerization, which arrested when the light source was turned off.

There are several other examples of photocatalytic polymerization pathways, using a variety of photosensitizers including iridium[126–128], iron[99], gold[92], and copper.[124]

5. Conclusion

We have summarized recent developments in metal-based photosensitizers and their applications in photocatalysis. Current research primarily focuses on enlarging the potential window of photosensitizers, using coordination-chemistry approaches. Beyond redox potentials, other important attributes of photosensitizers include photostability and long excited-state lifetimes, both of which are critical for the performance in photocatalytic applications. Electrochemical and photophysical characterization, in concert with Stern–Volmer quenching studies, can be used to evaluate a candidate photosensitizer before applying it in a photocatalytic reaction and allow for quantitative cataloging of all important photosensitizer attributes. That said, there is no "one size fits all" photosensitizer available, and the characteristics that are most important depend on the specific photoreaction that is being targeted. This has led to the development of a large variety of photosensitizer structures, using many different transition metals and ligand sets. And while a large part of the photocatalysis community uses "off the shelf" photosensitizers to develop new synthetic applications of photocatalysis, coordination-chemistry and physical inorganic chemistry approaches for designing new and improved photosensitizers will still play an important role in the continued growth of photocatalysis as a synthetic method.

Acknowledgments

We thank the National Science Foundation (CHE-1846831) and the Welch Foundation (E-1887) for funding our research on photosensitizers and photocatalysis.

Funding

This work was supported by the National Science Foundation [CHE-1846831] and Welch Foundation [E-1887].

ORCID

Jong-Hwa Shon http://orcid.org/0000-0002-7930-4271
Thomas S. Teets http://orcid.org/0000-0002-7471-8467

References

[1] Lamansky, S.; Djurovich, P.; Murphy, D.; Abdel-Razzaq, F.; Lee, H.-E.; Adachi, C.; Burrows, P. E.; Forrest, S. R.; Thompson, M. E. Highly Phosphorescent Bis-Cyclometalated Iridium Complexes: Synthesis, Photophysical Characterization, and Use in Organic Light Emitting Diodes. *J. Am. Chem. Soc.* 2001, 123(18), 4304–4312. DOI: 10.1021/ja003693s.

[2] Yersin, H.; Rausch, A. F.; Czerwieniec, R.; Hofbeck, T.; Fischer, T. The Triplet State of Organo-Transition Metal Compounds. Triplet Harvesting and Singlet Harvesting for Efficient OLEDs. *Coord. Chem. Rev.* 2011, 255(21–22), 2622–2652. DOI: 10.1016/j.ccr.2011.01.042.

[3] You, Y.; Cho, S.; Nam, W. Cyclometalated Iridium(III) Complexes for Phosphorescence Sensing of Biological Metal Ions. *Inorg. Chem.* 2014, 53(4), 1804–1815. DOI: 10.1021/ic4013872.

[4] Ma, D.-L.; Ma, V. P.-Y.; Chan, D. S.-H.; Leung, K.-H.; He, H.-Z.; Leung, C.-H. Recent Advances in Luminescent Heavy Metal Complexes for Sensing. *Coord. Chem. Rev.* 2012, 256(23–24), 3087–3113. DOI: 10.1016/j.ccr.2012.07.005.

[5] Yi, X.; Yang, P.; Huang, D.; Zhao, J. Visible Light-Harvesting Cyclometalated Ir(III) Complexes With Pyreno[4,5-d]Imidazole C^N Ligands as Triplet Photosensitizers for Triplet–Triplet Annihilation Upconversion. *Dyes Pigm.* 2013, 96(1), 104–115. DOI: 10.1016/j.dyepig.2012.07.020.

[6] Yuan, Y.-J.; Zhang, J.-Y.; Yu, Z.-T.; Feng, J.-Y.; Luo, W.-J.; Ye, J.-H.; Zou, Z.-G. Impact of Ligand Modification on Hydrogen Photogeneration and Light-Harvesting Applications Using Cyclometalated Iridium Complexes. *Inorg. Chem.* 2012, 51(7), 4123–4133. DOI: 10.1021/ic202423y.

[7] Cook, T. R.; Dogutan, D. K.; Reece, S. Y.; Surendranath, Y.; Teets, T. S.; Nocera, D. G. Solar Energy Supply and Storage for the Legacy and Nonlegacy Worlds. *Chem. Rev.* 2010, 110(11), 6474–6502. DOI: 10.1021/cr100246c.

[8] Ahmad, S.; Guillén, E.; Kavan, L.; Grätzel, M.; Nazeeruddin, M. K. Metal Free Sensitizer and Catalyst for Dye Sensitized Solar Cells. *Energy Environ. Sci.* 2013, 6 (12), 3439–3466. DOI: 10.1039/c3ee41888j.

[9] Wang, D.; Wu, Y.; Dong, H.; Qin, Z.; Zhao, D.; Yu, Y.; Zhou, G.; Jiao, B.; Wu, Z.; Gao, M., et al. Iridium (III) Complexes with 5,5-Dimethyl-3-(Pyridin-2-yl)Cyclohex-2-Enone Ligands as Sensitizer for Dye-Sensitized Solar Cells. *Org. Electron.* 2013, 14 (12), 3297–3305. DOI: 10.1016/j.orgel.2013.09.040.

[10] Yin, J.-F.; Velayudham, M.; Bhattacharya, D.; Lin, H.-C.; Lu, K.-L. Structure Optimization of Ruthenium Photosensitizers for Efficient Dye-Sensitized Solar Cells – A Goal toward A "Bright" Future. *Coord. Chem. Rev.* 2012, 256(23–24), 3008–3035. DOI: 10.1016/j.ccr.2012.06.022.

[11] Prier, C. K.; Rankic, D. A.; MacMillan, D. W. C. Visible Light Photoredox Catalysis with Transition Metal Complexes: Applications in Organic Synthesis. *Chem. Rev.* 2013, 113(7), 5322–5363. DOI: 10.1021/cr300503r.

[12] Corcoran, E. B.; Pirnot, M. T.; Lin, S.; Dreher, S. D.; DiRocco, D. A.; Davies, I. W.; Buchwald, S. L.; MacMillan, D. W. C. Aryl Amination Using Ligand-Free Ni(II) Salts and Photoredox Catalysis. *Science.* 2016, 353(6296), 279–283. DOI: 10.1126/science.aag0209.

[13] Cismesia, M. A.; Yoon, T. P. Characterizing Chain Processes in Visible Light Photoredox Catalysis. *Chem. Sci.* 2015, 6(10), 5426–5434. DOI: 10.1039/C5SC02185E.

[14] Lin, S.; Ischay, M. A.; Fry, C. G.; Yoon, T. P. Radical Cation Diels–Alder Cycloadditions by Visible Light Photocatalysis. *J. Am. Chem. Soc.* 2011, 133(48), 19350–19353. DOI: 10.1021/ja2093579.

[15] Dai, C.; Narayanam, J. M. R.; Stephenson, C. R. J. Visible-Light-Mediated Conversion of Alcohols to Halides. *Nat. Chem.* 2011, 3(2), 140–145. DOI: 10.1038/nchem.949.

[16] Juris, A.; Balzani, V.; Barigelletti, F.; Campagna, S.; Belser, P.; Zelewsky, A. V. Ru(II) Polypyridine Complexes: Photophysics, Photochemistry, Electrochemistry, and

Chemiluminescence. *Coord. Chem. Rev.* 1988, 84, 85–277. DOI: 10.1016/0010-8545(88)80032-8.

[17] Haga, M.; Dodsworth, E. S.; Eryavec, G.; Seymour, P.; Lever, A. B. P. Luminescence Quenching of the Tris(2,2′-Bipyrazine)Ruthenium(II) Cation and Its Monoprotonated Complex. *Inorg. Chem.* 1985, 24(12), 1901–1906. DOI: 10.1021/ic00206a041.

[18] Marcus, R. A.;. Chemical and Electrochemical Electron-Transfer Theory. *Annu. Rev. Phys. Chem.* 1964, 15(1), 155–196. DOI: 10.1146/annurev.pc.15.100164.001103.

[19] Marcus, R. A.;. On the Theory of Oxidation-Reduction Reactions Involving Electron Transfer. I. *J. Chem. Phys.* 1956, 24(5), 966–978. DOI: 10.1063/1.1742723.

[20] Shon, J.-H.; Teets, T. S. Potent Bis-Cyclometalated Iridium Photoreductants with β-Diketiminate Ancillary Ligands. *Inorg. Chem.* 2017, 56(24), 15295–15303. DOI: 10.1021/acs.inorgchem.7b02859.

[21] Shon, J.-H.; Sittel, S.; Teets, T. S. Synthesis and Characterization of Strong Cyclometalated Iridium Photoreductants for Application in Photocatalytic Aryl Bromide Hydrodebromination. *ACS Catal.* 2019, 9(9), 8646–8658. DOI: 10.1021/acscatal.9b02759.

[22] Murakami, M.; Ohkubo, K.; Fukuzumi, S. Inter- and Intramolecular Photoinduced Electron Transfer of Flavin Derivatives with Extremely Small Reorganization Energies. *Chem. - Eur. J.* 2010, 16(26), 7820–7832. DOI: 10.1002/chem.200903236.

[23] Albani, J. R.;. Chapter 4 - Fluorescence Quenching. In *Structure and Dynamics of Macromolecules: Absorption and Fluorescence Studies*; Albani, J. R., Ed.; Elsevier Science: Amsterdam, 2004; pp 141–192. DOI: 10.1016/B978-044451449-3/50004-6.

[24] Arias-Rotondo, D. M.; McCusker, J. K. The Photophysics of Photoredox Catalysis: A Roadmap for Catalyst Design. *Chem. Soc. Rev.* 2016, 45(21), 5803–5820. DOI: 10.1039/C6CS00526H.

[25] Kleinschmidt, M.; van Wüllen, C.; Marian, C. M. Intersystem-Crossing and Phosphorescence Rates in Fac-$Ir^{III}(Ppy)_3$: A Theoretical Study Involving Multi-Reference Configuration Interaction Wavefunctions. *J. Chem. Phys.* 2015, 142 (9), 094301. DOI: 10.1063/1.4913513.

[26] Ghosh, I.; Shaikh, R. S.; König, B. Sensitization-Initiated Electron Transfer for Photoredox Catalysis. *Angew. Chem. Int. Ed.* 2017, 56(29), 8544–8549. DOI: 10.1002/anie.201703004.

[27] Marchini, M.; Bergamini, G.; Cozzi, P. G.; Ceroni, P.; Balzani, V. Photoredox Catalysis: The Need to Elucidate the Photochemical Mechanism. *Angew. Chem. Int. Ed.* 2017, 56 (42), 12820–12821. DOI: 10.1002/anie.201706217.

[28] Zhao, W.; Castellano, F. N. Upconverted Emission from Pyrene and Di- *Tert* -butylpyrene Using $Ir(Ppy)_3$ as Triplet Sensitizer. *J. Phys. Chem. A*. 2006, 110(40), 11440–11445. DOI: 10.1021/jp064261s.

[29] Montalti, M.; Murov, S. L., Eds.. *Handbook of Photochemistry*. 3rded.; CRC/Taylor & Francis: Boca Raton, 2006.

[30] Rillema, D. P.; Allen, G.; Meyer, T. J.; Conrad, D. Redox Properties of Ruthenium(II) Tris Chelate Complexes Containing the Ligands 2,2′-bipyrazine, 2,2′-bipyridine, and 2,2′-bipyrimidine. *Inorg. Chem.* 1983, 22(11), 1617–1622. DOI: 10.1021/ic00153a012.

[31] Pham, P. V.; Nagib, D. A.; MacMillan, D. W. C. Photoredox Catalysis: A Mild, Operationally Simple Approach to the Synthesis of α-Trifluoromethyl Carbonyl Compounds. *Angew. Chem. Int. Ed.* 2011, 50(27), 6119–6122. DOI: 10.1002/anie.201101861.

[32] Bock, C. R.; Connor, J. A.; Gutierrez, A. R.; Meyer, T. J.; Whitten, D. G.; Sullivan, B. P.; Nagle, J. K. Estimation of Excited-State Redox Potentials by Electron-Transfer

Quenching. Application of Electron-Transfer Theory to Excited-State Redox Processes. *J. Am. Chem. Soc.* 1979, 101(17), 4815–4824. DOI: 10.1021/ja00511a007.

[33] Wallentin, C.-J.; Nguyen, J. D.; Finkbeiner, P.; Stephenson, C. R. J. Visible Light-Mediated Atom Transfer Radical Addition via Oxidative and Reductive Quenching of Photocatalysts. *J. Am. Chem. Soc.* 2012, 134(21), 8875–8884. DOI: 10.1021/ja300798k.

[34] Tucker, J. W.; Zhang, Y.; Jamison, T. F.; Stephenson, C. R. J. Visible-Light Photoredox Catalysis in Flow. *Angew. Chem. Int. Ed.* 2012, 51(17), 4144–4147. DOI: 10.1002/anie.201200961.

[35] Kalyanasundaram, K.;. Photophysics, Photochemistry and Solar Energy Conversion with Tris(Bipyridyl)Ruthenium(II) and Its Analogues. *Coord. Chem. Rev.* 1982, 46, 159–244. DOI: 10.1016/0010-8545(82)85003-0.

[36] Connelly, N. G.; Geiger, W. E. Chemical Redox Agents for Organometallic Chemistry. *Chem. Rev.* 1996, 96(2), 877–910. DOI: 10.1021/cr940053x.

[37] Tyson, E. L.; Niemeyer, Z. L.; Yoon, T. P. Redox Mediators in Visible Light Photocatalysis: Photocatalytic Radical Thiol–Ene Additions. *J. Org. Chem.* 2014, 79 (3), 1427–1436. DOI: 10.1021/jo500031g.

[38] Maity, S.; Zhu, M.; Shinabery, R. S.; Zheng, N. Intermolecular [3+2] Cycloaddition of Cyclopropylamines with Olefins by Visible-Light Photocatalysis. *Angew. Chem. Int. Ed.* 2012, 51(1), 222–226. DOI: 10.1002/anie.201106162.

[39] Iqbal, N.; Jung, J.; Park, S.; Cho, E. J. Controlled Trifluoromethylation Reactions of Alkynes through Visible-Light Photoredox Catalysis. *Angew. Chem.* 2014, 126(2), 549–552. DOI: 10.1002/ange.201308735.

[40] Oh, S. H.; Malpani, Y. R.; Ha, N.; Jung, Y.-S.; Han, S. B. Vicinal Difunctionalization of Alkenes: Chlorotrifluoromethylation with CF_3SO_2Cl by Photoredox Catalysis. *Org. Lett.* 2014, 16(5), 1310–1313. DOI: 10.1021/ol403716t.

[41] Dedeian, K.; Djurovich, P. I.; Garces, F. O.; Carlson, G.; Watts, R. J. A New Synthetic Route to the Preparation of A Series of Strong Photoreducing Agents: Fac-Tris-Ortho-Metalated Complexes of Iridium(III) with Substituted 2-phenylpyridines. *Inorg. Chem.* 1991, 30(8), 1685–1687. DOI: 10.1021/ic00008a003.

[42] Kim, H.; Kim, T.; Lee, D. G.; Roh, S. W.; Lee, C. Nitrogen-Centered Radical-Mediated C–H Imidation of Arenes and Heteroarenes via Visible Light Induced Photocatalysis. *Chem. Commun.* 2014, 50(66), 9273–9276. DOI: 10.1039/C4CC03905J.

[43] Nguyen, J. D.; D'Amato, E. M.; Narayanam, J. M. R.; Stephenson, C. R. J. Engaging Unactivated Alkyl, Alkenyl and Aryl Iodides in Visible-Light-Mediated Free Radical Reactions. *Nat. Chem.* 2012, 4(10), 854–859. DOI: 10.1038/nchem.1452.

[44] Teegardin, K.; Day, J. I.; Chan, J.; Weaver, J. Advances in Photocatalysis: A Microreview of Visible Light Mediated Ruthenium and Iridium Catalyzed Organic Transformations. *Org. Process Res. Dev.* 2016, 20(7), 1156–1163. DOI: 10.1021/acs.oprd.6b00101.

[45] Senaweera, S.; Weaver, J. D. Dual C–F, C–H Functionalization via Photocatalysis: Access to Multifluorinated Biaryls. *J. Am. Chem. Soc.* 2016, 138(8), 2520–2523. DOI: 10.1021/jacs.5b13450.

[46] Nacsa, E. D.; MacMillan, D. W. C. Spin-Center Shift-Enabled Direct Enantioselective α-Benzylation of Aldehydes with Alcohols. *J. Am. Chem. Soc.* 2018, 140(9), 3322–3330. DOI: 10.1021/jacs.7b12768.

[47] Guo, X.; Okamoto, Y.; Schreier, M. R.; Ward, T. R.; Wenger, O. S. Enantioselective Synthesis of Amines by Combining Photoredox and Enzymatic Catalysis in a Cyclic Reaction Network. *Chem. Sci.* 2018, 9(22), 5052–5056. DOI: 10.1039/C8SC01561A.

[48] Kerzig, C.; Guo, X.; Wenger, O. S. Unexpected Hydrated Electron Source for Preparative Visible-Light Driven Photoredox Catalysis. *J. Am. Chem. Soc.* 2019, 141 (5), 2122–2127. DOI: 10.1021/jacs.8b12223.

[49] Le, C.; MacMillan, D. W. C. A Radical Approach to the Copper Oxidative Addition Problem: Trifluoromethylation of Bromoarenes. *Science*. 2018, 360(6392), 1010–1014. DOI: 10.1126/science.aat4133.

[50] Zhang, P.; Le, C. C.; MacMillan, D. W. C. Silyl Radical Activation of Alkyl Halides in Metallaphotoredox Catalysis: A Unique Pathway for Cross-Electrophile Coupling. *J. Am. Chem. Soc.* 2016, 138(26), 8084–8087. DOI: 10.1021/jacs.6b04818.

[51] Kautzky, J. A.; Wang, T.; Evans, R. W.; MacMillan, D. W. C. Decarboxylative Trifluoromethylation of Aliphatic Carboxylic Acids. *J. Am. Chem. Soc.* 2018, 140(21), 6522–6526. DOI: 10.1021/jacs.8b02650.

[52] Beatty, J. W.; Stephenson, C. R. J. Amine Functionalization via Oxidative Photoredox Catalysis: Methodology Development and Complex Molecule Synthesis. *Acc. Chem. Res.* 2015, 48(5), 1474–1484. DOI: 10.1021/acs.accounts.5b00068.

[53] Nguyen, J. D.; Reiß, B.; Dai, C.; Stephenson, C. R. J. Batch to Flow Deoxygenation Using Visible Light Photoredox Catalysis. *Chem. Commun.* 2013, 49(39), 4352–4354. DOI: 10.1039/C2CC37206A.

[54] Devery, J. J.; Nguyen, J. D.; Dai, C.; Stephenson, C. R. J. Light-Mediated Reductive Debromination of Unactivated Alkyl and Aryl Bromides. *ACS Catal.* 2016, 6(9), 5962–5967. DOI: 10.1021/acscatal.6b01914.

[55] Finkenzeller, W. J.; Yersin, H. Emission of Ir(Ppy)3. Temperature Dependence, Decay Dynamics, and Magnetic Field Properties. *Chem. Phys. Lett.* 2003, 377(3–4), 299–305. DOI: 10.1016/S0009-2614(03)01142-4.

[56] Hofbeck, T.; Yersin, H. The Triplet State of *Fac* -Ir(ppy) $_3$. *Inorg. Chem.* 2010, 49(20), 9290–9299. DOI: 10.1021/ic100872w.

[57] Cheng, Y.; Gu, X.; Li, P. Visible-Light Photoredox in Homolytic Aromatic Substitution: Direct Arylation of Arenes with Aryl Halides. *Org. Lett.* 2013, 15(11), 2664–2667. DOI: 10.1021/ol400946k.

[58] Khaled, M. B.; El Mokadem, R. K.; Weaver, J. D. Hydrogen Bond Directed Photocatalytic Hydrodefluorination: Overcoming Electronic Control. *J. Am. Chem. Soc.* 2017, 139(37), 13092–13101. DOI: 10.1021/jacs.7b06847.

[59] Slinker, J. D.; Gorodetsky, A. A.; Lowry, M. S.; Wang, J.; Parker, S.; Rohl, R.; Bernhard, S.; Malliaras, G. G. Efficient Yellow Electroluminescence from a Single Layer of a Cyclometalated Iridium Complex. *J. Am. Chem. Soc.* 2004, 126(9), 2763–2767. DOI: 10.1021/ja0345221.

[60] Goldsmith, J. I.; Hudson, W. R.; Lowry, M. S.; Anderson, T. H.; Bernhard, S. Discovery and High-Throughput Screening of Heteroleptic Iridium Complexes for Photoinduced Hydrogen Production. *J. Am. Chem. Soc.* 2005, 127(20), 7502–7510. DOI: 10.1021/ja0427101.

[61] Nguyen, J. D.; Matsuura, B. S.; Stephenson, C. R. J. A Photochemical Strategy for Lignin Degradation at Room Temperature. *J. Am. Chem. Soc.* 2014, 136(4), 1218–1221. DOI: 10.1021/ja4113462.

[62] Lowry, M. S.; Goldsmith, J. I.; Slinker, J. D.; Rohl, R.; Pascal, R. A. Single-Layer Electroluminescent Devices and Photoinduced Hydrogen Production from an Ionic Iridium(III) Complex. *Chem. Mater.* 2005, 17, 5712–5719.

[63] Kim, H.; Lee, C. Visible-Light-Induced Photocatalytic Reductive Transformations of Organohalides. *Angew. Chem. Int. Ed.* 2012, 51(49), 12303–12306. DOI: 10.1002/anie.201203599.

[64] Erdmann, E.; Villinger, A.; König, B.; Seidel, W. W. 1,10-phenanthroline-dithiine Iridium and Ruthenium Complexes: Synthesis, Characterization and Photocatalytic Dihydrogen Evolution. *Photochem. Photobiol. Sci.* 2018, 17(8), 1056–1067. DOI: 10.1039/C8PP00068A.

[65] Whang, D. R.; Sakai, K.; Park, S. Y. Highly Efficient Photocatalytic Water Reduction with Robust Iridium(III) Photosensitizers Containing Arylsilyl Substituents. *Angew. Chem. Int. Ed.* 2013, 52(44), 11612–11615. DOI: 10.1002/anie.201305684.

[66] Takizawa, S.; Ikuta, N.; Zeng, F.; Komaru, S.; Sebata, S.; Murata, S. Impact of Substituents on Excited-State and Photosensitizing Properties in Cationic Iridium(III) Complexes with Ligands of Coumarin 6. *Inorg. Chem.* 2016, 55(17), 8723–8735. DOI: 10.1021/acs.inorgchem.6b01279.

[67] Yu, Z.-T.; Yuan, Y.-J.; Cai, J.-G.; Zou, Z.-G. Charge-Neutral Amidinate-Containing Iridium Complexes Capable of Efficient Photocatalytic Water Reduction. *Chem. - Eur. J.* 2013, 19(4), 1303–1310. DOI: 10.1002/chem.201203029.

[68] Tinker, L. L.; Bernhard, S. Photon-Driven Catalytic Proton Reduction with a Robust Homoleptic Iridium(III) 6-phenyl-2,2′-bipyridine Complex ($[ir(c^{\wedge}n^{\wedge}n)_2]^+$). *Inorg. Chem.* 2009, 48(22), 10507–10511. DOI: 10.1021/ic900777g.

[69] Sato, S.; Morikawa, T.; Kajino, T.; Ishitani, O. A Highly Efficient Mononuclear Iridium Complex Photocatalyst for CO_2 Reduction under Visible Light. *Angew. Chem. Int. Ed.* 2013, 52(3), 988–992. DOI: 10.1002/anie.201206137.

[70] DiSalle, B. F.; Bernhard, S. Orchestrated Photocatalytic Water Reduction Using Surface-Adsorbing Iridium Photosensitizers. *J. Am. Chem. Soc.* 2011, 133(31), 11819–11821. DOI: 10.1021/ja201514e.

[71] Shon, J.-H.; Teets, T. S. Molecular Photosensitizers in Energy Research and Catalysis: Design Principles and Recent Developments. *ACS Energy Lett.* 2019, 4(2), 558–566. DOI: 10.1021/acsenergylett.8b02388.

[72] Lim, B. S.; Rahtu, A.; Gordon, R. G. Atomic Layer Deposition of Transition Metals. *Nat. Mater.* 2003, 2(11), 749–754. DOI: 10.1038/nmat1000.

[73] Liu, Y.; Ye, K.; Fan, Y.; Song, W.; Wang, Y.; Hou, Z. Amidinate-Ligated Iridium(III) Bis(2-Pyridyl)Phenyl Complex as an Excellent Phosphorescent Material for Electroluminescence Devices. *Chem. Commun.* 2009, 25, 3699–3701. DOI: 10.1039/b902807b.

[74] Choi, J.; MacArthur, A. H. R.; Brookhart, M.; Goldman, A. S. Dehydrogenation and Related Reactions Catalyzed by Iridium Pincer Complexes. *Chem. Rev.* 2011, 111(3), 1761–1779. DOI: 10.1021/cr1003503.

[75] Polson, M.; Fracasso, S.; Bertolasi, V.; Ravaglia, M.; Scandola, F. Iridium Cyclometalated Complexes with Axial Symmetry. Synthesis and Photophysical Properties of a *Trans* -biscyclometalated Complex Containing the Terdentate Ligand 2,6-diphenylpyridine. *Inorg. Chem.* 2004, 43(6), 1950–1956. DOI: 10.1021/ic0351848.

[76] Whittle, V. L.; Williams, J. A. G. A New Class of Iridium Complexes Suitable for Stepwise Incorporation into Linear Assemblies: Synthesis, Electrochemistry, and Luminescence. *Inorg. Chem.* 2008, 47(15), 6596–6607. DOI: 10.1021/ic701788d.

[77] Du, P.; Schneider, J.; Jarosz, P.; Eisenberg, R. Photocatalytic Generation of Hydrogen from Water Using a Platinum(II) Terpyridyl Acetylide Chromophore. *J. Am. Chem. Soc.* 2006, 128(24), 7726–7727. DOI: 10.1021/ja0610683.

[78] Du, P.; Schneider, J.; Jarosz, P.; Zhang, J.; Brennessel, W. W.; Eisenberg, R. Photoinduced Electron Transfer in Platinum(II) Terpyridyl Acetylide Chromophores: Reductive and Oxidative Quenching and Hydrogen Production †. *J. Phys. Chem. B.* 2007, 111(24), 6887–6894. DOI: 10.1021/jp072187n.

[79] Hua, F.; Kinayyigit, S.; Cable, J. R.; Castellano, F. N. Platinum(II) Diimine Diacetylides: Metallacyclization Enhances Photophysical Properties. *Inorg. Chem.* 2006, 45(11), 4304–4306. DOI: 10.1021/ic060102b.

[80] Choi, W. J.; Choi, S.; Ohkubo, K.; Fukuzumi, S.; Cho, E. J.; You, Y. Mechanisms and Applications of Cyclometalated Pt(II) Complexes in Photoredox Catalytic Trifluoromethylation. *Chem. Sci.* 2015, 6(2), 1454–1464. DOI: 10.1039/C4SC02537G.

[81] Mydlak, M.; Mauro, M.; Polo, F.; Felicetti, M.; Leonhardt, J.; Diener, G.; De Cola, L.; Strassert, C. A. Controlling Aggregation in Highly Emissive Pt(II) Complexes Bearing Tridentate Dianionic N □ N □ N Ligands. Synthesis, Photophysics, and Electroluminescence. *Chem. Mater.* 2011, 23(16), 3659–3667. DOI: 10.1021/cm2010902.

[82] Yam, V. W. W.; Tang, R. P.L.; Wong, K. M. C.; Cheung, K. K. Synthesis, Luminescence, Electrochemistry, and Ion-Binding Studies of Platinum(II) Terpyridyl Acetylide Complexes. *Organometallics*. 2001, 20(22), 4476–4482. DOI: 10.1021/om010336x.

[83] Yang, Q.-Z.; Wu, L.-Z.; Wu, Z.-X.; Zhang, L.-P.; Tung, C.-H. Long-Lived Emission from Platinum(II) Terpyridyl Acetylide Complexes. *Inorg. Chem.* 2002, 41(22), 5653–5655. DOI: 10.1021/ic025580a.

[84] Hissler, M.; McGarrah, J. E.; Connick, W. B.; Geiger, D. K.; Cummings, S. D.; Eisenberg, R. Platinum Diimine Complexes: Towards a Molecular Photochemical Device. *Coord. Chem. Rev.* 2000, 208, 115–137. DOI: 10.1016/S0010-8545(00)00254-X.

[85] Schneider, J.; Du, P.; Jarosz, P.; Lazarides, T.; Wang, X.; Brennessel, W. W.; Eisenberg, R. Cyclometalated 6-phenyl-2,2′-bipyridyl (CNN) Platinum(II) Acetylide Complexes: Structure, Electrochemistry, Photophysics, and Oxidative- and Reductive-Quenching Studies. *Inorg. Chem.* 2009, 48(10), 4306–4316. DOI: 10.1021/ic801947v.

[86] Zhang, Y.; Lee, T. S.; Petersen, J. L.; Milsmann, C. A Zirconium Photosensitizer with A Long-Lived Excited State: Mechanistic Insight into Photoinduced Single-Electron Transfer. *J. Am. Chem. Soc.* 2018, 140(18), 5934–5947. DOI: 10.1021/jacs.8b00742.

[87] Büldt, L. A.; Guo, X.; Prescimone, A.; Wenger, O. S. A molybdenum(0) Isocyanide Analogue of Ru(2,2′-Bipyridine)$_3^{2+}$: A Strong Reductant for Photoredox Catalysis. *Angew. Chem. Int. Ed.* 2016, 55(37), 11247–11250. DOI: 10.1002/anie.201605571.

[88] Sattler, W.; Henling, L. M.; Winkler, J. R.; Gray, H. B. Bespoke Photoreductants: Tungsten Arylisocyanides. *J. Am. Chem. Soc.* 2015, 137(3), 1198–1205. DOI: 10.1021/ja510973h.

[89] Kern, J.-M.; Sauvage, J.-P. Photoassisted C–C Coupling via Electron Transfer to Benzylic Halides by a Bis(Di-Imine) Copper(I) Complex. *J. Chem. Soc. Chem. Commun.* 1987, 8, 546–548. DOI: 10.1039/C39870000546.

[90] Pirtsch, M.; Paria, S.; Matsuno, T.; Isobe, H.; Reiser, O. [Cu(dap)$_2$cl] as an Efficient Visible-Light-Driven Photoredox Catalyst in Carbon-Carbon Bond-Forming Reactions. *Chem. - Eur. J.* 2012, 18(24), 7336–7340. DOI: 10.1002/chem.201200967.

[91] Kjær, K. S.; Kaul, N.; Prakash, O.; Chábera, P.; Rosemann, N. W.; Honarfar, A.; Gordivska, O.; Fredin, L. A.; Bergquist, K.-E.; Häggström, L., et al. Luminescence and Reactivity of a Charge-Transfer Excited Iron Complex with Nanosecond Lifetime. *Science*. 2019, 363(6424), 249–253. DOI: 10.1126/science.aau7160.

[92] Nzulu, F.; Telitel, S.; Stoffelbach, F.; Graff, B.; Morlet-Savary, F.; Lalevée, J.; Fensterbank, L.; Goddard, J.-P.; Ollivier, C. A. Dinuclear Gold(I) Complex as a Novel Photoredox Catalyst for Light-Induced Atom Transfer Radical Polymerization. *Polym. Chem.* 2015, 6(25), 4605–4611. DOI: 10.1039/C5PY00435G.

[93] Whittemore, T. J.; Millet, A.; Sayre, H. J.; Xue, C.; Dolinar, B. S.; White, E. G.; Dunbar, K. R.; Turro, C. Tunable Rh $_2$ (II,II) Light Absorbers as Excited-State

Electron Donors and Acceptors Accessible with Red/Near-Infrared Irradiation. *J. Am. Chem. Soc.* 2018, 140(15), 5161–5170. DOI: 10.1021/jacs.8b00599.

[94] Hockin, B. M.; Li, C.; Robertson, N.; Zysman-Colman, E. Photoredox Catalysts Based on Earth-Abundant Metal Complexes. *Catal. Sci. Technol.* 2019, 9(4), 889–915. DOI: 10.1039/C8CY02336K.

[95] Francés-Monerris, A.; Gros, P. C.; Assfeld, X.; Monari, A.; Pastore, M. Toward Luminescent Iron Complexes: Unravelling the Photophysics by Computing Potential Energy Surfaces. *ChemPhotoChem.* 2019, 3(9), 666–683. DOI: 10.1002/cptc.201900100.

[96] Cai, S.; Zhao, X.; Wang, X.; Liu, Q.; Li, Z.; Wang, D. Z. Visible-Light-Promoted C–C Bond Cleavage: Photocatalytic Generation of Iminium Ions and Amino Radicals. *Angew. Chem. Int. Ed.* 2012, 51(32), 8050–8053. DOI: 10.1002/anie.201202880.

[97] Cheng, Y.; Yang, J.; Qu, Y.; Li, P. Aerobic Visible-Light Photoredox Radical C–H Functionalization: Catalytic Synthesis of 2-substituted Benzothiazoles. *Org. Lett.* 2012, 14(1), 98–101. DOI: 10.1021/ol2028866.

[98] McNally, A.; Prier, C. K.; MacMillan, D. W. C. Discovery of an -amino C-H Arylation Reaction Using the Strategy of Accelerated Serendipity. *Science.* 2011, 334(6059), 1114–1117. DOI: 10.1126/science.1213920.

[99] Pan, X.; Malhotra, N.; Zhang, J.; Matyjaszewski, K. Photoinduced Fe-Based Atom Transfer Radical Polymerization in the Absence of Additional Ligands, Reducing Agents, and Radical Initiators. *Macromolecules.* 2015, 48(19), 6948–6954. DOI: 10.1021/acs.macromol.5b01815.

[100] Pac, C.; Ihama, M.; Yasuda, M.; Miyauchi, Y.; Sakurai, H. Tris(2,2′-Bipyridine) Ruthenium(2+)-Mediated Photoreduction of Olefins with 1-Benzyl-1,4-Dihydronicotinamide: A Mechanistic Probe for Electron-Transfer Reactions of NAD(P)H-Model Compounds. *J. Am. Chem. Soc.* 1981, 103(21), 6495–6497. DOI: 10.1021/ja00411a040.

[101] Du, J.; Yoon, T. P. Crossed Intermolecular [2+2] Cycloadditions of Acyclic Enones via Visible Light Photocatalysis. *J. Am. Chem. Soc.* 2009, 131(41), 14604–14605. DOI: 10.1021/ja903732v.

[102] Tyson, E. L.; Farney, E. P.; Yoon, T. P. Photocatalytic [2 + 2] Cycloadditions of Enones with Cleavable Redox Auxiliaries. *Org. Lett.* 2012, 14(4), 1110–1113. DOI: 10.1021/ol3000298.

[103] Torres, J.; Carrión, M. C.; Leal, J.; Jalón, F. A.; Cuevas, J. V.; Rodríguez, A. M.; Castañeda, G.; Manzano, B. R. Cationic Bis(Cyclometalated) Ir(III) Complexes with Pyridine–Carbene Ligands. Photophysical Properties and Photocatalytic Hydrogen Production from Water. *Inorg. Chem.* 2018, 57(3), 970–984. DOI: 10.1021/acs.inorgchem.7b02289.

[104] Bachmann, C.; Guttentag, M.; Spingler, B.; Alberto, R. 3d Element Complexes of Pentadentate Bipyridine-Pyridine-Based Ligand Scaffolds: Structures and Photocatalytic Activities. *Inorg. Chem.* 2013, 52(10), 6055–6061. DOI: 10.1021/ic4004017.

[105] Du, P.; Schneider, J.; Li, F.; Zhao, W.; Patel, U.; Castellano, F. N.; Eisenberg, R. Bi- and Terpyridyl Platinum(II) Chloro Complexes: Molecular Catalysts for the Photogeneration of Hydrogen from Water or Simply Precursors for Colloidal Platinum? *J. Am. Chem. Soc.* 2008, 130(15), 5056–5058. DOI: 10.1021/ja711090w.

[106] Petronilho, A.; Woods, J. A.; Bernhard, S.; Albrecht, M. Bimetallic Iridium-Carbene Complexes with Mesoionic Triazolylidene Ligands for Water Oxidation Catalysis: Bimetallic Iridium-Carbene Complexes. *Eur. J. Inorg. Chem.* 2014, 2014(4), 708–714. DOI: 10.1002/ejic.201300843.

[107] Woods, J. A.; Lalrempuia, R.; Petronilho, A.; McDaniel, N. D.; Müller-Bunz, H.; Albrecht, M.; Bernhard, S. Carbene Iridium Complexes for Efficient Water Oxidation: Scope and Mechanistic Insights. *Energy Env. Sci.* 2014, 7(7), 2316–2328. DOI: 10.1039/C4EE00971A.

[108] Li, M.; Takada, K.; Goldsmith, J. I.; Bernhard, S. Iridium(III) Bis-Pyridine-2-Sulfonamide Complexes as Efficient and Durable Catalysts for Homogeneous Water Oxidation. *Inorg. Chem.* 2016, 55(2), 518–526. DOI: 10.1021/acs.inorgchem.5b01709.

[109] Han, Z.; Qiu, F.; Eisenberg, R.; Holland, P. L.; Krauss, T. D. Robust Photogeneration of H_2 in Water Using Semiconductor Nanocrystals and a Nickel Catalyst. *Science*. 2012, 338(6112), 1321–1324. DOI: 10.1126/science.1227775.

[110] Metz, S.; Bernhard, S. Robust Photocatalytic Water Reduction with Cyclometalated Ir(III) 4-vinyl-2,2′-bipyridine Complexes. *Chem. Commun.* 2010, 46(40), 7551–7553. DOI: 10.1039/c0cc01827a.

[111] Tinker, L. L.; McDaniel, N. D.; Curtin, P. N.; Smith, C. K.; Ireland, M. J.; Bernhard, S. Visible Light Induced Catalytic Water Reduction without an Electron Relay. *Chem. - Eur. J.* 2007, 13(31), 8726–8732. DOI: 10.1002/chem.200700480.

[112] Teets, T. S.; Nocera, D. G. Photocatalytic Hydrogen Production. *Chem. Commun.* 2011, 47(33), 9268–9274. DOI: 10.1039/c1cc12390d.

[113] Cheung, P. L.; Machan, C. W.; Malkhasian, A. Y. S.; Agarwal, J.; Kubiak, C. P. Photocatalytic Reduction of Carbon Dioxide to CO and HCO_2H Using *Fac*-$Mn(CN)(Bpy)(CO)_3$. *Inorg. Chem.* 2016, 55(6), 3192–3198. DOI: 10.1021/acs.inorgchem.6b00379.

[114] Morris, A. J.; Meyer, G. J.; Fujita, E. Molecular Approaches to the Photocatalytic Reduction of Carbon Dioxide for Solar Fuels. *Acc. Chem. Res.* 2009, 42(12), 1983–1994. DOI: 10.1021/ar9001679.

[115] Seo, H.; Katcher, M. H.; Jamison, T. F. Photoredox Activation of Carbon Dioxide for Amino Acid Synthesis in Continuous Flow. *Nat. Chem.* 2016, 9(5), 453–456. DOI: 10.1038/nchem.2690.

[116] Takeda, H.; Cometto, C.; Ishitani, O.; Robert, M. Electrons, Photons, Protons and Earth-Abundant Metal Complexes for Molecular Catalysis of CO_2 Reduction. *ACS Catal.* 2017, 7(1), 70–88. DOI: 10.1021/acscatal.6b02181.

[117] Chen, L.; Guo, Z.; Wei, X.-G.; Gallenkamp, C.; Bonin, J.; Anxolabéhère-Mallart, E.; Lau, K.-C.; Lau, T.-C.; Robert, M. Molecular Catalysis of the Electrochemical and Photochemical Reduction of CO_2 with Earth-Abundant Metal Complexes. Selective Production of CO Vs HCOOH by Switching of the Metal Center. *J. Am. Chem. Soc.* 2015, 137(34), 10918–10921. DOI: 10.1021/jacs.5b06535.

[118] Genoni, A.; Chirdon, D. N.; Boniolo, M.; Sartorel, A.; Bernhard, S.; Bonchio, M. Tuning Iridium Photocatalysts and Light Irradiation for Enhanced CO_2 Reduction. *ACS Catal.* 2017, 7(1), 154–160. DOI: 10.1021/acscatal.6b03227.

[119] Thoi, V. S.; Kornienko, N.; Margarit, C. G.; Yang, P.; Chang, C. J. Visible-Light Photoredox Catalysis: Selective Reduction of Carbon Dioxide to Carbon Monoxide by a Nickel *N* -heterocyclic Carbene–Isoquinoline Complex. *J. Am. Chem. Soc.* 2013, 135(38), 14413–14424. DOI: 10.1021/ja4074003.

[120] Bosque, I.; Magallanes, G.; Rigoulet, M.; Kärkäs, M. D.; Stephenson, C. R. J. Redox Catalysis Facilitates Lignin Depolymerization. *ACS Cent. Sci.* 2017, 3(6), 621–628. DOI: 10.1021/acscentsci.7b00140.

[121] Kärkäs, M. D.; Matsuura, B. S.; Monos, T. M.; Magallanes, G.; Stephenson, C. R. J. Transition-Metal Catalyzed Valorization of Lignin: The Key to a Sustainable

Carbon-Neutral Future. *Org. Biomol. Chem.* 2016, 14(6), 1853–1914. DOI: 10.1039/C5OB02212F.

[122] Li, C.; Zhao, X.; Wang, A.; Huber, G. W.; Zhang, T. Catalytic Transformation of Lignin for the Production of Chemicals and Fuels. *Chem. Rev.* 2015, 115(21), 11559–11624. DOI: 10.1021/acs.chemrev.5b00155.

[123] Zhang, J.; Jiang, X.; Ye, X.; Chen, L.; Lu, Q.; Wang, X.; Dong, C. Pyrolysis Mechanism of A β-O-4 Type Lignin Dimer Model Compound: A Joint Theoretical and Experimental Study. *J. Therm. Anal. Calorim.* 2016, 123(1), 501–510. DOI: 10.1007/s10973-015-4944-y.

[124] Yang, Q.; Dumur, F.; Morlet-Savary, F.; Poly, J.; Lalevée, J. Photocatalyzed Cu-Based ATRP Involving an Oxidative Quenching Mechanism under Visible Light. *Macromolecules*. 2015, 48(7), 1972–1980. DOI: 10.1021/ma502384y.

[125] Fors, B. P.; Hawker, C. J. Control of a Living Radical Polymerization of Methacrylates by Light. *Angew. Chem. Int. Ed.* 2012, 51(35), 8850–8853. DOI: 10.1002/anie.201203639.

[126] Lalevée, J.; Peter, M.; Dumur, F.; Gigmes, D.; Blanchard, N.; Tehfe, M.-A.; Morlet-Savary, F.; Fouassier, J. P. Subtle Ligand Effects in Oxidative Photocatalysis with Iridium Complexes: Application to Photopolymerization. *Chem. Eur. J.* 2011, 17(52), 15027–15031. DOI: 10.1002/chem.201101445.

[127] Lalevée, J.; Tehfe, M.-A.; Dumur, F.; Gigmes, D.; Blanchard, N.; Morlet-Savary, F.; Fouassier, J. P. Iridium Photocatalysts in Free Radical Photopolymerization under Visible Lights. *ACS Macro Lett.* 2012, 1(2), 286–290. DOI: 10.1021/mz2001753.

[128] Telitel, S.; Dumur, F.; Telitel, S.; Soppera, O.; Lepeltier, M.; Guillaneuf, Y.; Poly, J.; Morlet-Savary, F.; Fioux, P.; Fouassier, J.-P., et al. Photoredox Catalysis Using a New Iridium Complex as an Efficient Toolbox for Radical, Cationic and Controlled Polymerizations under Soft Blue to Green Lights. *Polym. Chem.* 2015, 6(4), 613–624. DOI: 10.1039/C4PY01358A.